JAK inhibition decreases the autoimmune burden in Down syndrome

Author list: Angela L. Rachubinski[1,2*], Elizabeth Wallace[3], Emily Gurnee[3], Belinda A. Enriquez Estrada[1], Kayleigh R. Worek[1], Keith P. Smith[1], Paula Araya[1], Katherine A. Waugh[1,4], Ross E. Granrath[1], Eleanor Britton[1], Hannah R. Lyford[1], Micah G. Donovan[1,5], Neetha Paul Eduthan[1], Amanda A. Hill[1], Barry Martin[6], Kelly D. Sullivan[1,7], Lina Patel[1,8], Deborah J. Fidler[9], Matthew D. Galbraith[1,5], Cory A. Dunnick[3], David A. Norris[3], Joaquin M. Espinosa[1,5*].

Affiliations:

[1]Linda Crnic Institute for Down Syndrome, University of Colorado Anschutz Medical Campus, Aurora, CO, USA.

[2]Department of Pediatrics, Section of Developmental Pediatrics, University of Colorado Anschutz Medical Campus, Aurora, CO, USA.

[3]Department of Dermatology, University of Colorado Anschutz Medical Campus, Aurora, CO, USA.

[4]Current address: Department of Cell Biology and Physiology, University of Kansas Medical Center, Kansas City, KS, USA.

[5]Department of Pharmacology, University of Colorado Anschutz Medical Campus, Aurora, CO, USA

[6]Department of Internal Medicine, University of Colorado Anschutz Medical Campus, Aurora, CO, USA.

[7]Department of Pediatrics, Section of Developmental Biology, University of Colorado Anschutz Medical Campus, Aurora, CO, USA.

[8]Department of Psychiatry, Child and Adolescent Division, University of Colorado Anschutz Medical Campus, Aurora, CO, USA.

[9]Department of Human Development and Family Studies, Colorado State University, Fort Collins, CO, USA.

*Corresponding authors:

joaquin.espinosa@cuanschutz.edu / angela.rachubinski@cuanschutz.edu

Abstract.

Individuals with Down syndrome (DS), the genetic condition caused by trisomy 21 (T21), display clear signs of immune dysregulation, including high rates of autoimmune disorders and severe complications from infections. Although it is well established that T21 causes increased interferon responses and JAK/STAT signaling, elevated autoantibodies, global immune remodeling, and hypercytokinemia, the interplay between these processes, the clinical manifestations of DS, and potential therapeutic interventions remain ill defined. Here, we report a comprehensive analysis of immune dysregulation at the clinical, cellular, and molecular level in hundreds of individuals with DS. We demonstrate multi-organ autoimmunity of pediatric onset concurrent with unexpected autoantibody-phenotype associations. Importantly, constitutive immune remodeling and hypercytokinemia occur from an early age prior to autoimmune diagnoses or autoantibody production. We then report the interim analysis of a Phase II clinical trial investigating the safety and efficacy of the JAK inhibitor tofacitinib through multiple clinical and molecular endpoints. Analysis of the first 10 participants to complete the 16-week study shows a good safety profile and no serious adverse events. Treatment reduced skin pathology in alopecia areata, psoriasis, and atopic dermatitis, while decreasing interferon scores, cytokine scores, and levels of pathogenic autoantibodies without overt immune suppression. Additional research is needed to define the effects of JAK inhibition on the broader developmental and clinical hallmarks of DS. ClinicalTrials.gov identifier: NCT04246372.

46 **Introduction.**

47 Trisomy of human chromosome 21 (T21) occurs at a rate of ~1 in 700 live births, causing Down
48 syndrome (DS)[1,2]. Individuals with DS display a distinct clinical profile including developmental delays,
49 stunted growth, cognitive impairments, and increased risk of leukemia, autism spectrum disorders, seizure
50 disorders, and Alzheimer's disease[2,3]. People with DS also display widespread immune dysregulation,
51 which manifests through severe complications from respiratory viral infections and high prevalence of
52 myriad immune conditions, including autoimmune thyroid disease (AITD)[4-6], celiac disease[7,8], and skin
53 conditions such as atopic dermatitis, alopecia areata, hidradenitis suppurativa (HS), vitiligo, and psoriasis[9-
54 11]. Furthermore, people with DS display signs of neuroinflammation from an early age[12-14]. Although it is
55 now well accepted that immune dysregulation is a hallmark of DS, the underlying mechanisms and
56 therapeutic implications are not yet fully defined.

57 We previously reported that T21 causes consistent activation of the interferon (IFN) transcriptional
58 response in multiple immune and non-immune cell types with concurrent hypersensitivity to IFN
59 stimulation and hyperactivation of downstream JAK/STAT signaling[15-17]. Plasma proteomics studies
60 identified dozens of inflammatory cytokines with mechanistic links to IFN signaling that are elevated in
61 people with DS[18]. A large metabolomics study revealed that T21 drives the production of neurotoxic
62 tryptophan catabolites via the IFN-inducible kynurenine pathway[19]. Deep immune profiling revealed
63 global immune remodeling with hypersensitivity to IFN across all major branches of the immune system[15],
64 and dysregulation of T cell lineages toward a hyperactive, autoimmunity-prone state[16]. These results could
65 be partly explained by the fact that four of the six IFN receptors (IFNRs) are encoded on chr21, including
66 Type I, II and III IFNR subunits[20]. In a mouse model of DS, normalization of *IFNR* gene copy number
67 rescues multiple phenotypes of DS, including lethal immune hypersensitivity, congenital heart defects
68 (CHDs), cognitive impairments, and craniofacial anomalies[21]. JAK inhibition rescues lethal immune
69 hypersensitivity in these mouse models[22] and attenuates the global dysregulation of gene expression
70 caused by the trisomy across multiple murine tissues[23]. Furthermore, prenatal JAK inhibition in pregnant

71 mice prevents the appearance of CHDs[24]. Altogether, these results support the notion that T21 elicits an
72 interferonopathy in DS, and that pharmacological inhibition of IFN signaling could have multiple
73 therapeutic benefits in this population.

74 Although it is now well established that T21 disrupts immune homeostasis toward an autoimmunity-
75 prone state, the interplay between overexpression of chromosome 21 genes, hyperactive interferon
76 signaling, dysregulation of immune cell lineages, autoantibody production, hypercytokinemia, and the
77 various developmental and clinical features of DS remain to be elucidated. Previous studies established
78 similarities between the immune profiles of typical aging, autoimmunity in the general population, and
79 DS, proposing a role for accelerated immune aging in the pathophysiology of DS[25-27]. Other studies
80 indicate a role for elevated cytokine production, hyperactivated T cells, and ongoing B cell activation as
81 drivers of autoimmunity in DS[15,16,28]. However, given the relatively small sample sizes and observational
82 nature of these studies, it has not been possible to define the contribution of specific dysregulated events
83 to breach of tolerance leading to clinically evident autoimmunity in DS. Therefore, additional research is
84 needed to define driver versus bystander events that could illuminate therapeutic strategies to decrease the
85 burden of autoimmunity in DS.

86 Within this context, we report here a comprehensive analysis of the immune disorder of DS, including
87 detailed annotation of autoimmune and inflammatory conditions and quantification of autoantibodies in
88 hundreds of research participants, which reveals widespread autoimmune attack on all major organ
89 systems in DS from an early age, including unexpected autoantibody-phenotype associations. Then, using
90 deep immune mapping and quantitative proteomics, we demonstrate that T21 causes widespread immune
91 remodeling toward an autoimmunity-prone state accompanied by hypercytokinemia prior to clinically
92 evident autoimmunity or autoantibody production. Lastly, we report the interim analysis of a clinical trial
93 investigating the safety and efficacy of the JAK1/3 inhibitor tofacitinib (Xeljanz, Pfizer) in DS. These
94 results demonstrate that JAK inhibition improves multiple immunodermatological conditions in DS,
95 normalizes interferon scores, decreases levels of major pathogenic cytokines (e.g., TNF-α, IL-6), and

96 reduces levels of pathogenic autoantibodies [e.g., anti-thyroid peroxidase (anti-TPO)]. Altogether, these
97 results point to hyperactive JAK/STAT signaling as driver of autoimmunity in DS and justify the ongoing
98 trials of JAK inhibitors in DS for multiple clinical endpoints.
99

100 **Results.**

101 **Widespread multi-organ autoimmunity and autoantibody production in Down syndrome.**

102 Previous studies have documented increased rates of diverse autoimmune conditions in DS relative to
103 the general population including autoimmune thyroid disease (AITD)[29], celiac disease[30], autoimmune skin
104 conditions[9-11], and type I diabetes[31,32]. However, many of these studies were limited by relatively small
105 sample sizes, independent analysis of individual autoimmune conditions, or a focus on specific age ranges.
106 In order to complete a more comprehensive analysis of autoimmune conditions in DS across the lifespan,
107 we analyzed the harmonized clinical profiles of 441 research participants with DS, aged 6 months to 57
108 years, enrolled in the Human Trisome Project cohort study (HTP, NCT02864108), which annotates
109 clinical data through a combination of participant/caregiver surveys and expert abstraction of electronic
110 health records (EHRs) (see **Materials and Methods**, **Supplementary file 1**). In this analysis, the most
111 common autoimmune condition is AITD, affecting 53.1% of the total cohort (**Figure 1a**, **Figure 1 – figure**
112 **supplement 1a**). Grouped together, autoimmune and inflammatory skin conditions represent the second
113 most common category, affecting 43% of the cohort, including: atopic dermatitis / eczema (27.9%),
114 hidradenitis suppurativa / folliculitis / boils (20.6%), alopecia areata (7.7%), psoriasis (6.1%), and vitiligo
115 (1.9%) (**Figure 1a**, **Figure 1 - supplement 1b**). These observations align with recent epidemiological
116 studies demonstrating high rates of autoimmune and inflammatory skin conditions in DS[33,34]. The rate of
117 celiac disease (9.6%) is also highly elevated over that of the general population[35]. We observed 10 cases
118 (2.2%) of juvenile Type I diabetes, which has been reported to be more common in DS[31,32]. Other
119 autoimmune conditions common in the general population, such as systemic lupus erythematosus or
120 multiple sclerosis, were not observed in the HTP cohort. Other salient conditions annotated in this cohort
121 include recurrent otitis media (15.5%), frequent/recurrent pneumonia (9.2%), severe congenital heart
122 defects requiring surgical repair (19.5%), acute lymphocytic leukemia (ALL, 1.12%), and acute myeloid
123 leukemia (AML, 1.3%) (**Supplementary file 1**).

124 In the general population, the risk of autoimmune conditions increases with age and is higher in
125 females, with autoimmune conditions tending to cluster, whereby occurrence of one autoimmune
126 condition predisposes to a second condition[36,37]. Within the HTP cohort, analysis of age trajectories of
127 immune-related conditions in DS revealed early onset, with >80% of AITD, autoimmune/inflammatory
128 skin conditions, and celiac disease being diagnosed in the first two decades of life (**Figure 1 - supplement**
129 **1c-e**). The cumulative burden of autoimmunity and autoinflammation is similar in males versus females
130 with DS, albeit with slightly increased rates of AITD and hidradenitis suppurativa in females (**Figure 1 -**
131 **supplement 1f**). In terms of co-occurrence, when evaluating the adult population (18+ years old) for
132 AITD, autoimmune/inflammatory skin conditions and celiac disease, we found that 75% of participants
133 had a history of at least one condition, 38.4% had at least two, and 13.6% had three or more conditions
134 (**Figure 1b**).

135 Interestingly, analysis of medical records found an unexpectedly low number of individuals with
136 records of autoantibodies against the thyroid gland [4.3%, e.g., anti-thyroid peroxidase (TPO), anti-
137 thyroglobulin (TG)] within the HTP cohort (**Figure 1 - supplement 1a**). This could be explained by the
138 fact that thyroid disease is commonly diagnosed through measurements of thyroid-relevant hormones
139 (TSH, T3, T4) without concurrent testing of autoantibodies. To investigate further, we measured anti-TPO
140 levels as well as levels of anti-nuclear antibodies (ANA), a more general biomarker of autoimmunity
141 (**Supplementary file 2**). Remarkably, 82.4% of adults with DS show positivity for at least one of these
142 autoantibodies, with 41.2% being positive for both (**Figure 1c**). Indeed, 62% of individuals with history
143 of hypothyroidism were TPO+, whereby anti-TPO is just one of the possible autoantibodies associated
144 with AITD. Prompted by these results, we next completed a more comprehensive analysis of
145 autoantibodies in DS using protein array technology, with a focus on ~380 common autoepitopes from
146 270 proteins (see **Materials and Methods, Supplementary file 2**). These efforts identified 25
147 autoantibodies significantly over-represented in people with DS relative to age- and sex-matched controls
148 (**Figure 1d**), with 98.3% of individuals with DS being positive for at least one of these autoantibodies,

149 and 63.3% being positive for six or more (**Figure 1d-e**). In addition to autoantibodies against TPO, which
150 is expressed exclusively in the thyroid gland, we identified autoantibodies targeting proteins that are either
151 broadly expressed across multiple tissues (e.g., TOP1, UBA1, LAMP2) or preferentially expressed in
152 specific organs across the human body, including liver (e.g., CYP1A2), pancreas (e.g., SLC30A8), skin
153 (e.g., DSG3), bone marrow (e.g. SRP68), and brain tissue (e.g., AIMP1) (**Figure 1d, f**).

154 Analysis of autoantibody positivity relative to history of co-occurring conditions produced several
155 interesting observations. Expectedly, individuals with hypothyroidism are more likely to be positive for
156 anti-TPO antibodies (**Figure 1g-h**). However, unexpectedly, TPO+ status also associates with higher rates
157 of use of pressure equalizing (PE) tubes employed to alleviate the symptoms of recurrent ear infections
158 and otitis media with effusion (OME), which is common in DS[38] (**Figure 1g-h**). Possible interpretations
159 for this result are provided in the Discussion. Positivity for additional autoantibodies was more common
160 in those with other co-occurring neurological conditions, a broad classification encompassing various
161 seizure disorders, movement disorders, and structural brain abnormalities (**Figure 1g-h, Figure 1 – figure**
162 **supplement 1g**). Salient examples are antibodies against MUSK, a muscle-associated receptor tyrosine
163 kinase involved in clustering of the acetylcholine receptors in the neuromuscular junction[39]; UBA1, a
164 ubiquitin conjugating enzyme involved in antigen presentation[40]; and MYH6, a cardiac myosin heavy
165 chain isoform (**Figure 1g-h**, **Figure 1 – figure supplement 1g**). Individuals with history of tricuspid valve
166 regurgitation display higher rates of four different autoantibodies, most prominently against WARS1, a
167 tryptophan tRNA synthetase mutated in various neurodevelopmental disorders[41], and SRP68, a protein
168 commonly targeted by autoantibodies in necrotizing myopathies[42] (**Figure 1 – figure supplement 1g**).
169 Individuals with a history of frequent pneumonia present a higher frequency of autoantibodies against
170 DSG3 (desmoglein 3), a cell adhesion molecule targeted by autoantibodies in paraneoplastic pemphigus
171 (PNP), an autoimmune disease of the skin and mucous membranes that can involve fatal lung
172 complications[43] (**Figure 1g-h**).

173 Altogether, these results demonstrate widespread multi-organ autoimmunity across the lifespan in
174 people with DS, with production of multiple autoantibodies that could potentially contribute to a number
175 of co-occurring conditions more common in this population.
176

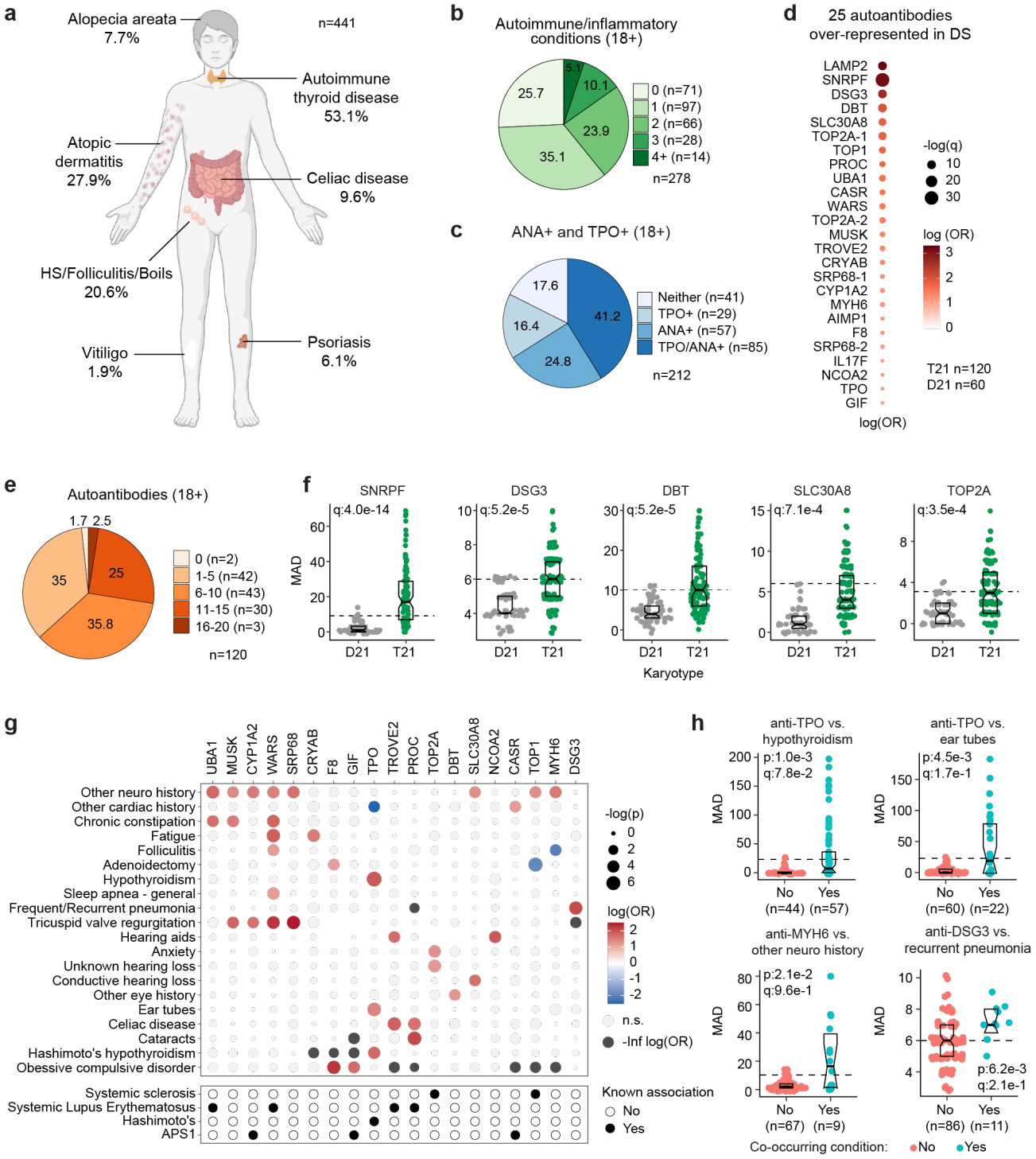

Figure 1. Multi-organ autoimmunity and widespread autoantibody production in Down syndrome. **a,** Overview of autoimmune and inflammatory conditions prevalent in persons with Down syndrome (DS) enrolled in the Human Trisome Project (HTP) cohort study. Percentages indicate the fraction of participants (n=441, all ages) with history of the indicated conditions. **b**, Pie chart showing

182 autoimmune/inflammatory condition burden in adults (n=278, 18+ years old) with DS. **c**, Pie chart
183 showing rates of positivity for anti-TPO and/or anti-nuclear antibodies (ANA) in adults (n=212, 18+ years
184 old) with DS. **d**, Bubble plot displaying odds-ratios and significance for 25 autoantibodies with elevated
185 rates of positivity in individuals with DS (n=120) versus 60 euploid controls (D21). q values calculated
186 by Benjamini-Hochberg adjustment of p-values from Fisher's exact test. **e**, Pie chart showing fractions of
187 adults with DS (n=120, 18+ years old) testing positive for various numbers of the autoantibodies identified
188 in d. **f**, Representative examples of autoantibodies more frequent in individuals with T21 (n=120) versus
189 euploid controls (D21, n=60). MAD: median absolute deviation. Dashed lines indicate the positivity
190 threshold of 90th percentile for D21. Data are presented as modified sina plots with boxes indicating
191 quartiles. **g**, Bubble plots showing the relationship between autoantibody positivity and history of various
192 clinical diagnoses in DS (n=120). Size of bubbles is proportional to -log-transformed p values from
193 Fisher's exact test. **h**, Sina plots displaying the levels of selected autoantibodies in individuals with DS
194 with or without the indicated co-occurring conditions. MAD: median absolute deviation. Dashed lines
195 indicate the positivity threshold of 90th percentile for D21. Sample sizes are indicated under each plot. q
196 values calculated by Benjamini-Hochberg adjustment of p-values from Fisher's exact tests.
197

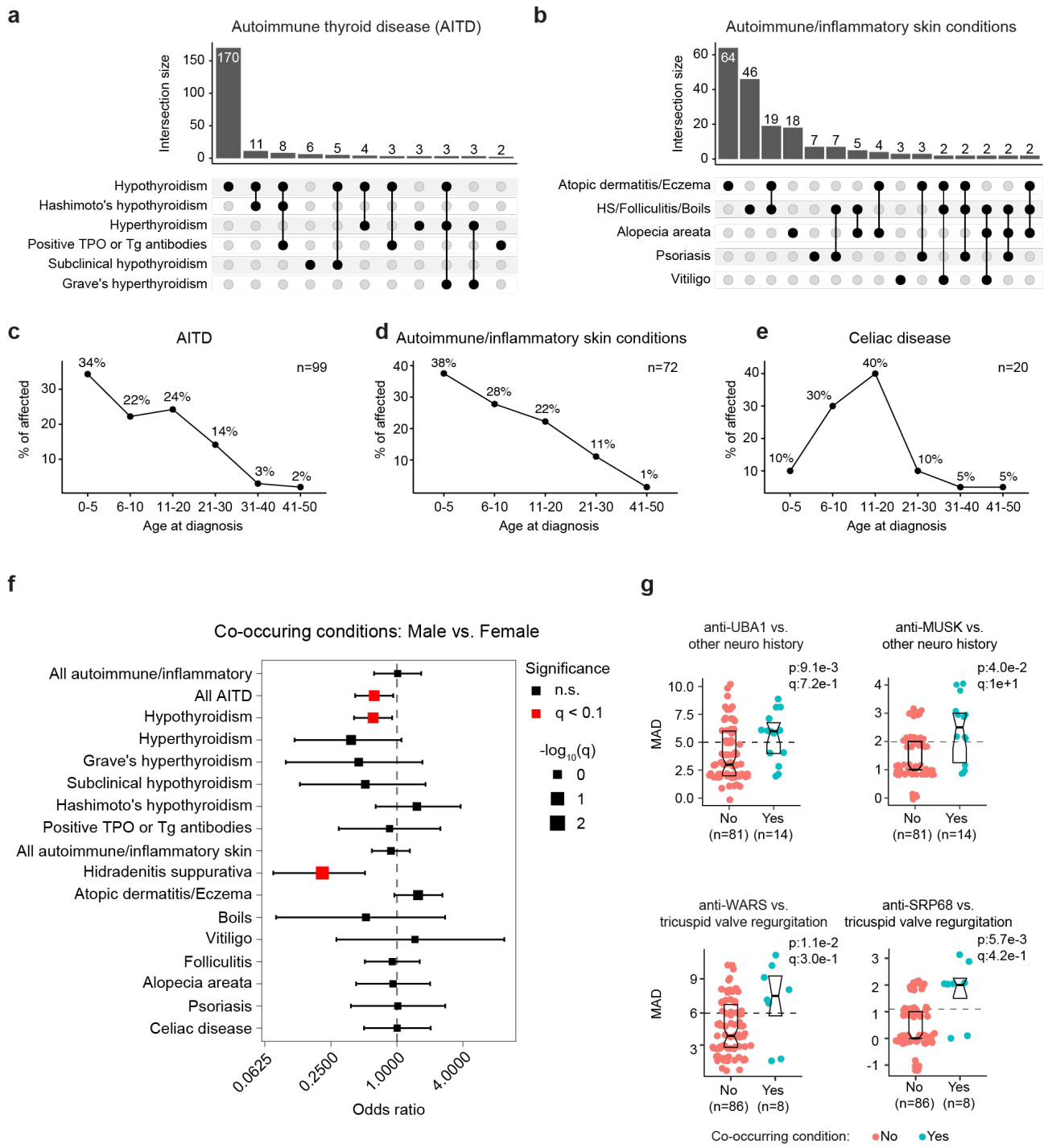

198

199 **Figure 1 – figure supplement 1. Early onset multi-organ autoimmunity and autoantibody**

200 **production in Down syndrome. a-b**, Upset plots showing overlap between various reported diagnoses

201 indicative of autoimmune thyroid disease (a) or autoimmune/inflammatory skin conditions (b) in research

202 participants with Down syndrome (DS, all ages, n=441) enrolled in the Human Trisome Project (HTP). **c-**

e, Plots showing the percentages of cases by age at diagnosis for AITD (c), autoimmune/inflammatory skin conditions (d), and celiac disease (e). Sample sizes indicated in each chart. **f**, Odds ratio plot for Fisher's exact test of proportions (cases vs. controls in males vs. females) for history of co-occurring conditions in individuals with DS (all ages, total n=441). Conditions with $q < 0.1$ (10% FDR) are highlighted in red. The size of square points is inversely proportional to q value; error bars represent 95% confidence intervals. **g**, Sina plots displaying the levels of select autoantibodies in individuals with DS, with or without history of the indicated co-occurring conditions. MAD: median absolute deviation. Horizontal dashed lines indicate 90th percentiles for the D21 group. Sample sizes are indicated under each plot. q values calculated by Benjamini-Hochberg adjustment of p-values from Fisher's exact tests.

213 **Trisomy 21 causes global immune remodeling regardless of evident clinical autoimmunity.**

214 Several immune cell changes have been proposed to underlie the autoimmunity-prone state of
215 DS[15,16,25,44], but specific immune cell-to-phenotype associations have not been established in previous
216 studies using smaller sample sizes. Therefore, we next investigated immune cell changes associated with
217 various clinical and molecular markers of autoimmunity in DS. Toward this end we analyzed mass
218 cytometry data from 292 individuals with DS relative to 96 euploid controls and tested for potential
219 differences in immune cell subpopulations, identified using FlowSOM[45], within the DS cohort based on
220 number of autoimmune/inflammatory disease diagnoses, ANA positivity, TPO positivity, and positivity
221 for additional autoantibodies. In agreement with previous analyses[15,16,25,44], we observed massive immune
222 remodeling in all major myeloid and lymphoid subsets, including increases in basophils, along with
223 depletion of eosinophils and total B cells (**Figure 2a-c, Figure 2 – figure supplement 1a-c**). When
224 comparing various subgroups within the DS cohort based on autoimmunity status, we observed that these
225 global immune changes are largely independent of the presence of clinical diagnoses or autoantibody
226 positivity, with very few additional changes significantly associated with these measures of autoimmunity
227 (**Figure 2 – figure supplement 1d**). For example, the significant depletion of B cells and enrichment of
228 basophils in DS is not significantly different among the various subgroups (**Figure 2c**, **Figure 2 – figure**
229 **supplement 1c**). Among CD45+ CD66^{lo} non-granulocytes, most changes are conserved among
230 subgroups, with the sole of exception of non-classical monocytes, which are further elevated in the ANA+
231 group (**Figure 2 – figure supplement 1d-e**). Among T cells, the overall pattern of depletion of naïve
232 subsets and enrichment of differentiated subsets characteristic of DS[15,16,28,44] is conserved across
233 subgroups, as illustrated by consistent depletion of CD8+ naïve subsets along with increases in the CD8+
234 terminally differentiated effector memory (TEMRA) subset (**Figure 2f, Figure 2 – figure supplement**
235 **1d**). Notably, we observed depletion of γδ T cells (both total and CD8+) in those with multiple
236 autoimmune diagnoses (**Figure 2 – figure supplement 1d, f**), a result that is in line with reports
237 documenting depletion of these subsets from peripheral circulation toward sites of active autoimmunity[46].

238 We also observed slight elevation of CD4+ T central memory cells (TCM) (**Figure 2 – figure supplement**
239 **1d, f**). Among B cells, the overall shift toward more differentiated states such as plasmablasts, age-
240 associated B cells (ABCs), and IgM+ memory cells is also conserved among subgroups, with the sole
241 exception of ABCs, which tend to be further elevated in the TPO+ group (**Figure 2g-i**, **Figure 2 – figure**
242 **supplement 1d, g**).

243 Altogether, these results indicate that T21 causes global remodeling of the immune system toward an
244 autoimmunity-prone and pro-inflammatory state, prior to clinically evident autoimmunity, and dwarfing
245 any additional effects associated with confirmed diagnoses of autoimmune/inflammatory conditions or
246 common biomarkers of autoimmunity.

247

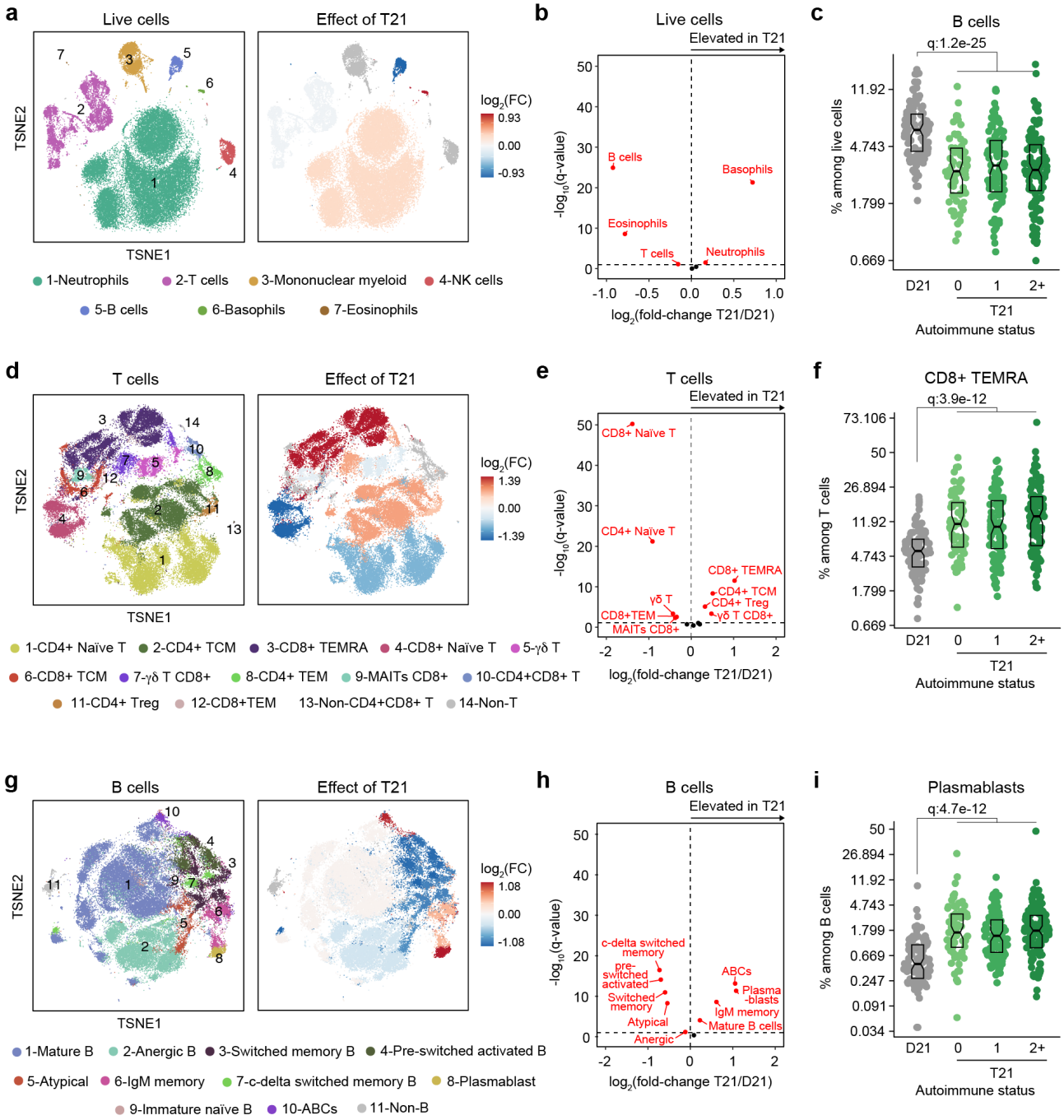

Figure 2. Trisomy 21 causes global immune remodeling regardless of clinically evident autoimmunity. a, t-distributed Stochastic Neighbor Embedding (t-SNE) plot displaying major immune populations identified by FlowSOM analysis of mass cytometry data for all live cells (left) and color coded by significant impact of T21 (beta regression q<0.1) on their relative frequency (right). Red indicates increased frequency and blue indicates decreased frequency among research participants with T21 (n=292) versus euploid controls (D21, n=96). **b**, Volcano plot showing the results of beta regression

255 analysis of major immune cell populations among all live cells in research participants with T21 (n=292)
256 versus euploid controls (D21, n=96). The dashed horizontal line indicates a significance threshold of
257 10% FDR (q<0.1) after Benjamini-Hochberg correction for multiple testing. **c**, Frequencies of B cells
258 among all live cells in euploid controls (D21, n=96) versus individuals with T21 and history of 0 (n=69),
259 1 (n=102) or 2+ (n=121) autoimmune/inflammatory conditions. Data is displayed as modified sina plots
260 with boxes indicating quartiles. **d-f**, Description as in a-c, but for subsets of T cells. **g-i**, Description as
261 in a-c, but for subsets of B cells.
262

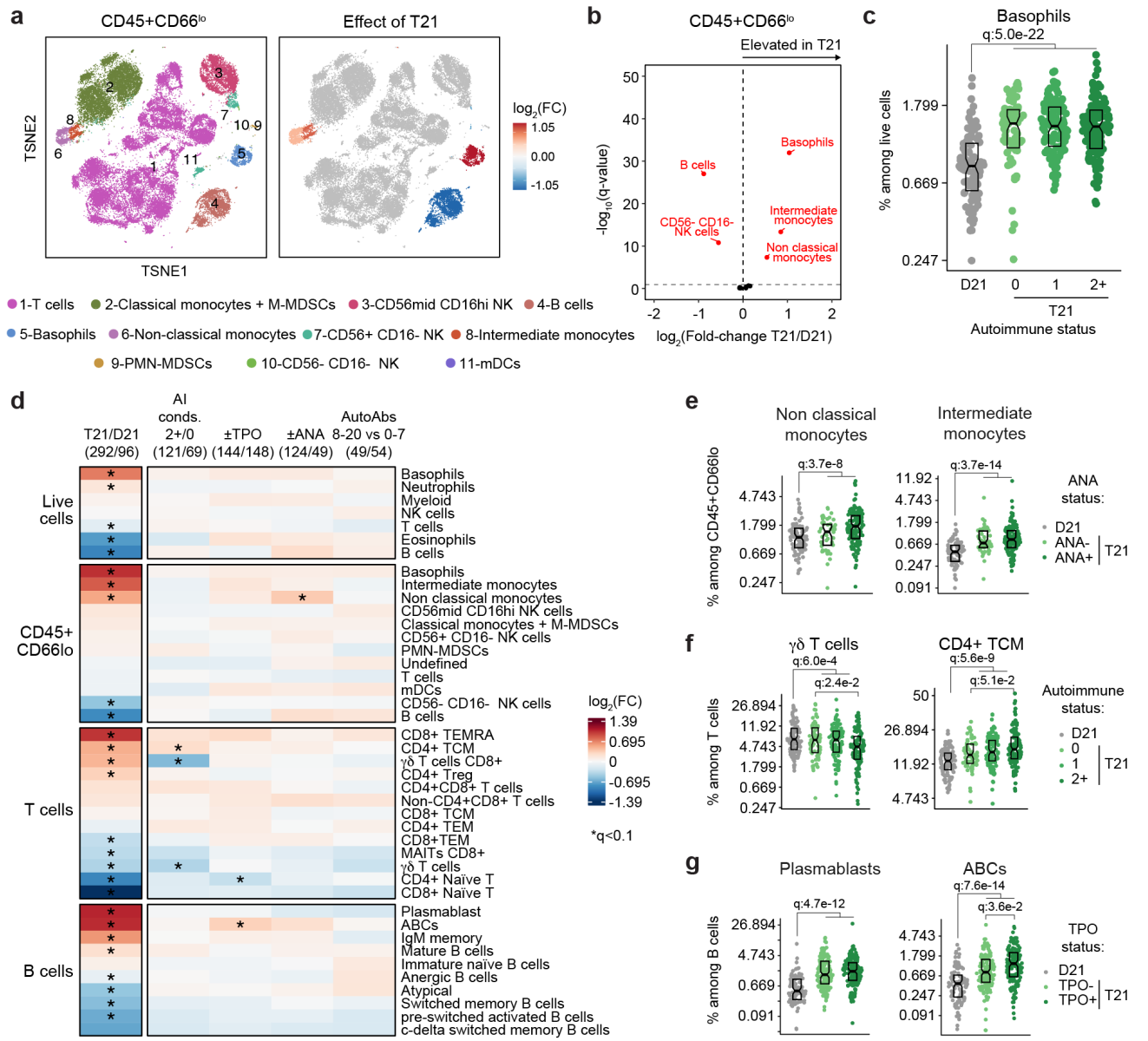

Figure 2 – figure supplement 1. Consistent remodeling of the peripheral immune system in Down syndrome. a, t-distributed Stochastic Neighbor Embedding (t-SNE) plot displaying major immune populations identified by FlowSOM analysis of mass cytometry data for CD45+ CD66^{lo} non-granulocytes (left) and color coded by the impact of trisomy 21 (T21) on their relative frequency (right). Red indicates increased frequency and blue indicates decreased frequency among research participants with T21 (n=292) versus euploid controls (D21, n=96). **b**, Volcano plot showing the results of beta regression analysis of immune cell populations among CD45+ CD66^{lo} non-granulocytes from research participants with T21 (n=292) versus euploid controls (D21, n=96). The dashed horizontal line indicates

272 a significance threshold of 10% FDR (q<0.1) after Benjamini-Hochberg correction for multiple testing.
273 **c**, Frequencies of basophils among all live cells in euploid controls (D21, n=96) versus individuals with
274 T21 and history of 0 (n=44), 1 (n=71) or 2+ (n=88) autoimmune/inflammatory conditions. Data is
275 displayed as modified sina plots with boxes indicating quartiles. **d**, Heatmap summarizing the results of
276 beta regression testing for differences in frequencies of indicated immune cell populations among all
277 live cells, CD45+ CD66^{lo} non-granulocytes, T cells, and B cells by T21 (n=292) versus D21 (n=96)
278 status, or by different subgroups within the T21 cohort: 2+ (n=88) versus 0 (n=44)
279 autoimmune/inflammatory conditions; TPO+ (n=144) versus TPO- (n=148); ANA+ (n=124) versus
280 ANA- (n=49); or positivity for 8-20 (n=49) versus 0-7 (n=54) autoantibodies elevated in DS. Asterisks
281 indicate significance after Benjamini-Hochberg correction for multiple testing (q<0.1, 10% FDR). **e-g**,
282 Representative examples of immune cell populations from d, showing effects of ANA positivity (e),
283 number of autoimmune conditions (f), and TPO status (g). Data are presented as modified sina plots
284 with boxes indicating quartiles, with q-values indicating beta regression significance after Benjamini-
285 Hochberg correction for multiple testing.
286

287 **Trisomy 21 causes hypercytokinemia from an early age independent of autoimmunity status.**

288 It is well established that individuals with DS display elevated levels of many inflammatory markers,
289 including several interleukins, cytokines, and chemokines known to drive autoimmune conditions, such
290 as IL-6 and TNF-α[18,28,44,47]. However, the interplay between hypercytokinemia, individual elevated
291 cytokines, and development of autoimmune conditions in DS remains to be elucidated. Therefore, we
292 analyzed data available from the HTP cohort for 54 inflammatory markers in plasma samples from 346
293 individuals with DS versus 131 euploid controls and cross-referenced these data with the presence of
294 autoimmune conditions and autoantibodies. These efforts confirmed the notion of profound
295 hypercytokinemia in DS[18,28,44,47], with significant elevation of multiple acute phase proteins (e.g. CRP,
296 SAA, IL1RA), pro-inflammatory cytokines (TSLP, IL-17C, IL-22, IL-17D, IL-9, IL-6, TNF-α) and
297 chemokines (IP-10, MIP-3a, MIP-1a, MCP-1, MCP-4, Eotaxin), as well as growth factors associated with
298 inflammation and wound healing (FGF, PlGF, VEGF-A) (**Figure 3a**). However, when evaluating for
299 differences within the DS cohort based on various metrics of autoimmunity, we did not observe important
300 differences based on number of autoimmune/inflammatory conditions, ANA or TPO positivity status, or
301 number of other autoantibodies (**Figure 3a**). For example, CRP, IL-6, and TNF-α are equally elevated
302 across all these subgroups (**Figure 3b-d, Figure 3 - figure supplement 1a**).

303 Previous studies have reported signs of early immunosenescence and inflammaging in DS, including
304 accelerated progression of immune lineages toward terminally differentiated states, early thymic atrophy,
305 and elevated levels of pro-inflammatory markers associated with age in the typical population[25,27,48,49].
306 However, the extent to which the inflammatory profile of DS represents accelerated ageing versus other
307 processes remains ill-defined. To address this, we first identified age-associated changes in immune
308 markers within the euploid and DS cohorts separately (**Figure 3 - figure supplement 1b-c**). This exercise
309 identified multiple immune markers that were up- or down-regulated with age, with an overall conserved
310 pattern of age trajectories in both groups (**Figure 3 - figure supplement 1c**). For example, increased age
311 is associated with increased CRP levels and decreased IL-17B levels in both cohorts (**Figure 3 - figure**

312 **supplement 1d**). We then compared the effects of age versus T21 status on cytokine levels in the DS
313 cohort, which identified many inflammatory factors elevated in DS across the lifespan that do not display
314 a significant increase with age, such as IL-9 and IL-17C, or that increase with age only in the DS cohort,
315 such as IP-10 (**Figure 3e-f, Figure 3 - figure supplement 1e**).
316 Altogether, these results indicate that T21 induces a constitutive hypercytokinemia from early
317 childhood, with only a fraction of these inflammatory changes being exacerbated with age.
318
319

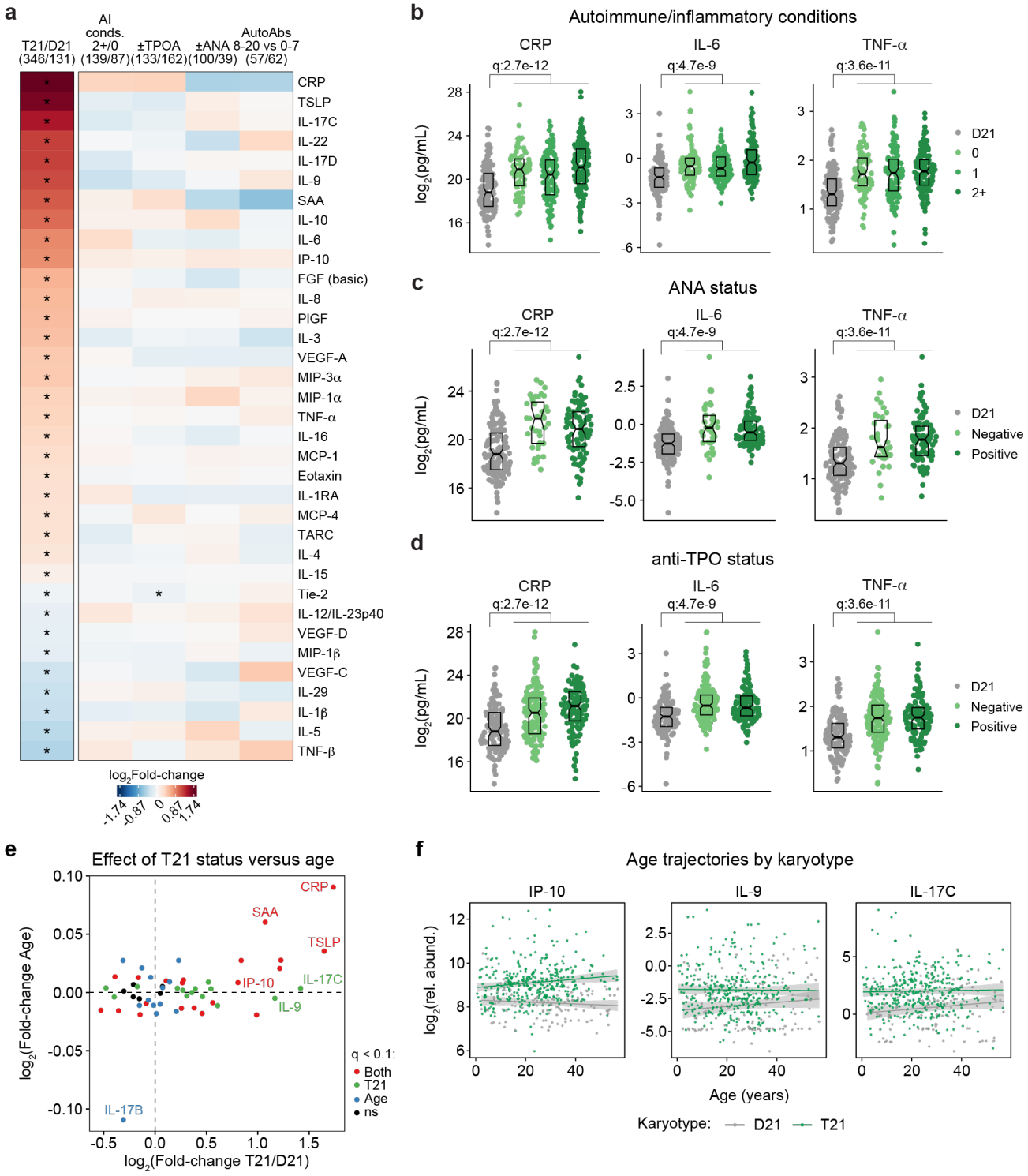

Figure 3. Trisomy 21 causes constitutive hypercytokinemia independent of autoimmunity status from an early age. a, Heatmap displaying $\log_2$-transformed fold-changes for plasma immune markers with significant differences in trisomy 21 (T21, n=346) versus euploid (D21, n=131), and between different subgroups within the T21 cohort: history of 2+ (n=139) versus 0 (n=87)

325 autoimmune/inflammatory conditions (AI conds.); TPO+ (n=133) versus TPO- (n=162); ANA+ (n=100)
326 versus ANA- (n=39); or positivity for 8-20 (n=57) versus 0-7 (n=62) autoantibodies (AutoAbs) elevated
327 in DS. Asterisks indicate linear regression significance after Benjamini-Hochberg correction for multiple
328 testing (q<0.1, 10% FDR). **b-d**, Comparison of CRP, IL-6 and TNF-α levels in euploid controls (D21,
329 n=131) versus subsets of individuals with T21 based on number of autoimmune/inflammatory
330 conditions (**b**), ANA positivity (**c**) or TPO positivity (**d**). Data are presented as modified sina plots with
331 boxes indicating quartiles. Samples sizes as in a. q-values indicate linear regression significance after
332 Benjamini-Hochberg correction for multiple testing. **e**, Scatter plot comparing the effect of T21
333 karyotype versus the effect of age in individuals with T21 (n=54 immune markers in 346 individuals
334 with T21), highlighting immune markers that are significantly different by T21 status, age, or both. ns:
335 not significantly different by T21 status or age. **f**, Scatter plots for example immune markers that are
336 significantly elevated in T21, but which are either not elevated with age in the euploid (D21) cohort (i.e.,
337 IP-10), or in either the T21 (n=346) or D21 (n=131) cohorts. Lines represent least-squares linear fits
338 with 95% confidence intervals in grey.
339

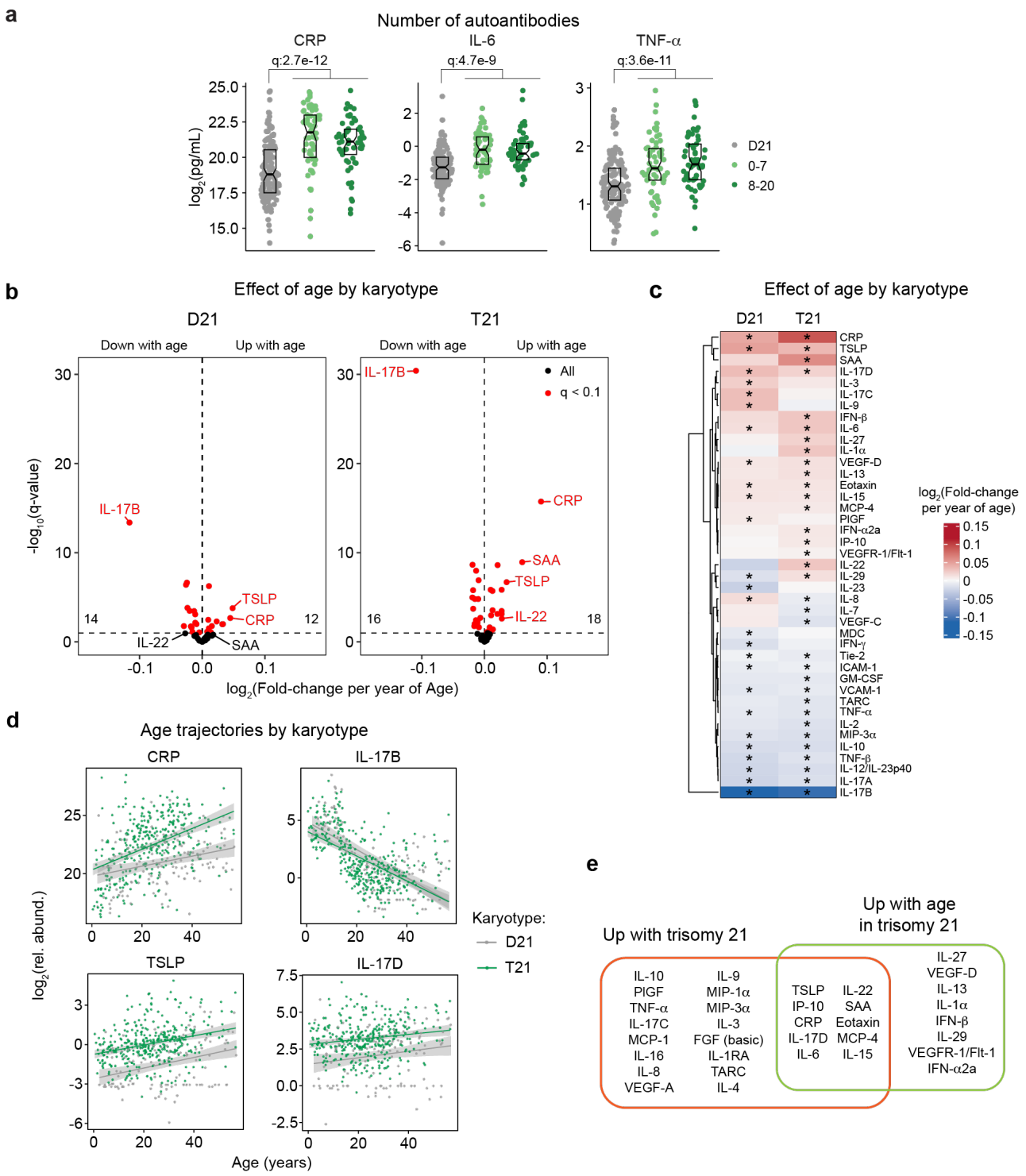

Figure 3 – figure supplement 1. Consistent hypercytokinemia from an early age in Down syndrome. a, Comparison of CRP, IL-6, and TNF-α levels in euploid controls (D21, n=131) versus subsets of individuals with T21 based on number of autoantibodies commonly elevated in Down syndrome: 0-7 autoantibodies (n=62) versus 8-20 autoantibodies (n=57). Data are presented as modified

345 sina plots with boxes indicating quartiles. q-values indicate linear regression significance after
346 Benjamini-Hochberg correction for multiple testing. **b**, Volcano plots presenting the results of linear
347 regression testing for association between age and the levels of 54 immune markers in the plasma of
348 euploid controls (left, D21, n=131) and individuals with trisomy 21 (right, T21, n=346) enrolled in the
349 Human Trisome Project (HTP) study. Horizontal dashed lines indicate a significance threshold of 10%
350 FDR ($q<0.1$) after Benjamini-Hochberg correction for multiple testing. **c**, Heatmap comparing the effect
351 of age on levels of immune markers in D21 and T21. Heatmap color scale represents log2-transformed
352 mean fold-change per year of age; asterisks indicate significance ($q < 0.1$) for linear regression testing.
353 **d**, Scatter plots showing the age trajectories of select immune markers in D21 versus T21. Sample sizes
354 as in c. Lines represent least squares linear fits with shaded areas indicating 95% confidence interval. **e**,
355 Diagram representing the overlap between immune markers elevated in T21 versus D21 and those
356 elevated with age in T21.

357

358 **A clinical trial for JAK inhibition in Down syndrome.**

359 Several lines of evidence support the notion that IFN hyperactivity and downstream JAK/STAT
360 signaling are key drivers of immune dysregulation in DS[15-19,22,24,44,50]. In mouse models of DS, both
361 normalization of *IFNR* gene copy number and pharmacologic JAK1 inhibition rescue their lethal immune
362 hypersensitivity phenotypes[22,50]. Furthermore, we recently demonstrated that IFN transcriptional scores
363 derived from peripheral immune cells correlate significantly with the degree of immune remodeling and
364 hypercytokinemia in DS[44], and we and others have reported the safe use of JAK inhibitors for treatment
365 of diverse immune conditions in DS, including alopecia areata[51], psoriatic arthritis[52] and hemophagocytic
366 lymphohistocytosis[53] through small case series. Encouraged by these results, we launched a clinical trial
367 to assess the safety and efficacy of the JAK inhibitor tofacitinib (Xeljanz, Pfizer) in DS, using moderate-
368 to-severe autoimmune/inflammatory skin conditions as a qualifying criterion (NCT04246372). This trial
369 is a single-site, open-label, Phase II clinical trial enrolling individuals with DS between the ages of 12 and
370 50 years old affected by alopecia areata, hidradenitis suppurativa, psoriasis, atopic dermatitis, or vitiligo
371 (see qualifying disease scores in **Supplementary file 3**). After screening, qualifying participants are
372 prescribed 5 mg of tofacitinib twice daily for 16 weeks, with an optional extension to 40 weeks (**Figure**
373 **4a**, see **Materials and Methods**). After enrollment and assessments at a baseline visit, participants attend
374 five safety monitoring visits during the main 16-week trial period. The recruitment goal for this trial is 40
375 participants who complete 16 weeks of tofacitinib treatment, with a predefined IRB-approved qualitative
376 interim analysis triggered when the first 10 participants completed the main 16-week trial (**Figure 4b**).
377 Among the first 13 participants enrolled, one participant withdrew shortly after enrollment, one was
378 excluded from analyses due to medication non-compliance (i.e., >15% missed doses), and one participant
379 had not yet completed the trial at the time of the interim analysis (**Figure 4b**). Demographic characteristics
380 of the 10 participants included in the interim analysis are shared in **Supplementary file 3**. Baseline
381 qualifying conditions of the 10 participants included in the interim analysis were alopecia areata (n=6),
382 hidradenitis suppurativa (n=3), and psoriasis (n=1) (open circles in **Figure 4c**). Two participants presented

383 with concurrent atopic dermatitis, two with concurrent vitiligo, and two with concurrent hidradenitis
384 suppurativa, albeit below the severity required to be the qualifying conditions (see closed circles in **Figure**
385 **4c**). In addition, seven participants had AITD/TPO+ and three had a celiac disease diagnosis (**Figure 4c**).
386

387 **Tofacitinib is well tolerated in Down syndrome.**

388 Analysis of adverse events (AEs) recorded for the 10 first participants over 16 weeks did not identify
389 any AEs considered definitely related to tofacitinib treatment or classified as severe. Several AEs were
390 annotated as 'possibly related' to treatment (**Figure 4d, Supplementary file 4**). Five episodes of upper
391 respiratory infections (URIs) affecting five different participants were observed. Based on the safety data
392 for tofacitinib in the general population[54], all episodes of URIs were annotated as possibly related to
393 treatment. Participant AA2 developed occasional cough and rhinorrhea that resolved with over-the-
394 counter medication. Two other participants reported transient rhinorrhea (AA3, AA5). Participant AA4
395 developed a nasal congestion, with chest pain and a productive cough. This participant tested negative for
396 SARS-Co-V2, Flu A-B, and RSV. Tofacitinib was not paused during this episode, and symptoms resolved
397 with over-the-counter medication. Participant HS2 experienced a sore throat with middle ear inflammation
398 that resolved with over-the-counter treatment. This participant also presented with folliculitis, which
399 resolved with antibiotic treatment. Participant HS1 experienced a short transient elevation (<3 days) in
400 creatine phosphokinase (CPK) that resolved spontaneously, and rash acneiform. Participant Ps1
401 experienced a transient and asymptomatic decrease in white blood cell (WBC) counts that resolved by the
402 end of the trial.

403 Overall**,** tofacitinib treatment was not discontinued for any of the 10 participants over the 16-week
404 study period, and seven participants eventually obtained off-label prescriptions after completing the trial
405 and are currently taking the medicine. Based on these interim results, recruitment resumed and is ongoing.
406

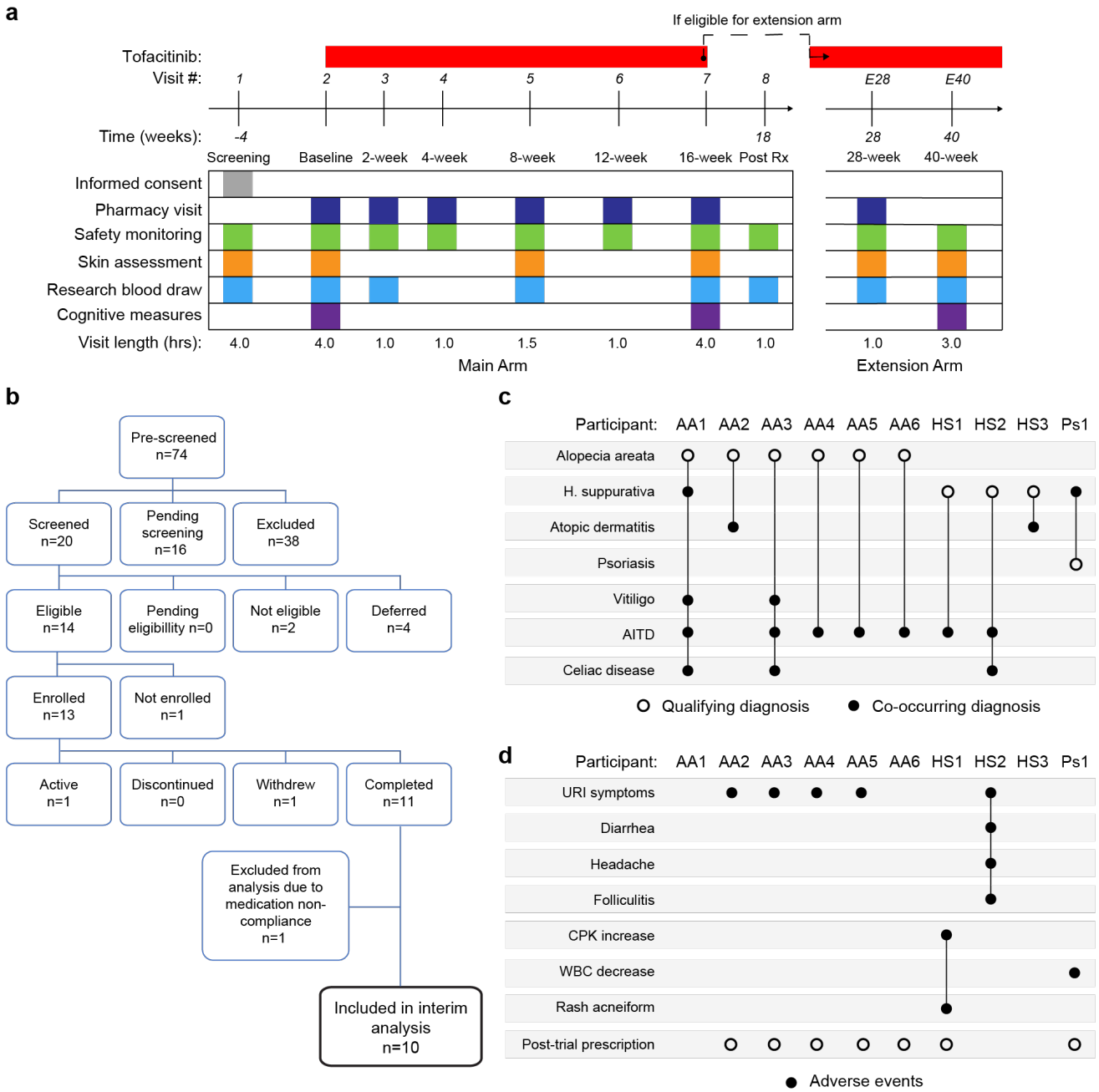

Figure 4. Clinical trial for JAK inhibition in Down syndrome. a, Schedule of activities for clinical trial of JAK inhibition in Down syndrome (NCT04246372). **b,** Consort chart for first 13 participants enrolled in the clinical trial. **c,** Upset plot displaying the qualifying and co-occurring autoimmune/inflammatory conditions for the 10 participants included in the interim analysis. **d,** Upset plots summarizing the adverse events annotated for the first 10 participants over a 16-week treatment period.

414 **Tofacitinib improves diverse autoimmune/inflammatory skin conditions in Down syndrome**.

415 In the clinical trial, skin pathology is monitored using global metrics of skin health, including the
416 Investigator's Global Assessment (IGA) and the Dermatology Life Quality Index (DLQI), as well as
417 disease-specific scores, such as the severity of alopecia tool (SALT), the psoriasis area and severity index
418 (PASI), or the eczema area and severity index (EASI) (see **Materials and Methods, Supplementary file**
419 **5**. The interim analysis showed that seven of the ten participants had an improvement in the IGA score
420 and eight of the ten reported some improvement on their life quality related to their skin condition as
421 measured by the DLQI (**Figure 5a-b**). The most striking effects were observed for alopecia areata (**Figure**
422 **5c-d, Figure 5 – figure supplement 1a**). Five of six participants with alopecia areata showed scalp hair
423 regrowth, with the exception being a male participant (AA1) with history of alopecia totalis for 20+ years
424 who only showed facial hair and eyelash re-growth. One participant presented with psoriasis due to
425 psoriatic arthritis and experienced an almost complete remission of psoriatic arthritis symptoms (Ps1,
426 **Figure 5 – figure supplement 1b-c**). For the two participants that presented with atopic dermatitis, the
427 clinical manifestations were markedly reduced during tofacitinib treatment (**Figure 5e-f**). A total of five
428 participants were affected by HS, three of them as the qualifying condition (HS1-3). No clear trend was
429 seen in the Modified Sartorius Scale (MSS) score used to monitor HS (**Figure 5 – figure supplement 1d-**
430 **e**).

431 Altogether, these results indicate that JAK inhibition could provide therapeutic benefit for several
432 autoimmune/inflammatory skin conditions more common in DS.

433

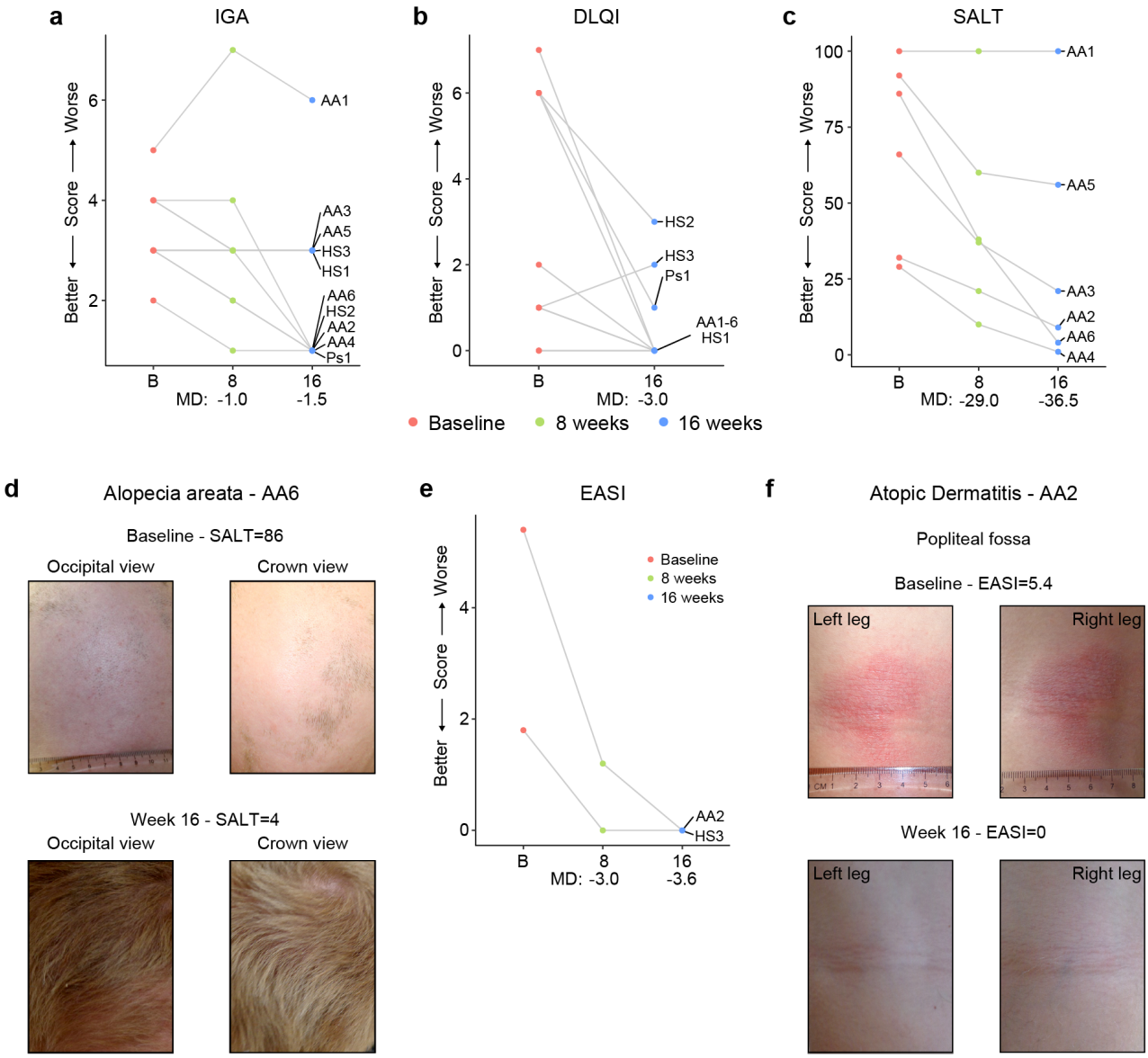

Figure 5. Tofacitinib improves diverse immune skin pathologies in Down syndrome. a-b, Investigator global assessment (IGA) scores (a) and Dermatological Life Quality Index (DLQI) scores (b) for the first 10 participants at baseline visit (B), mid-point (8 weeks) and endpoint (16 weeks) visits. MD: median difference. **c,** Severity of Alopecia Tool (SALT) scores for the first seven participants with alopecia areata in the trial. **d,** Images of participant AA6 at baseline versus week 16. **e,** Eczema Area and Severity Index (EASI) scores for two participants with mild atopic dermatitis. **f,** Images of participant AA2 showing improvement in atopic dermatitis upon tofacitinib treatment. p values not shown as per interim analysis plan.

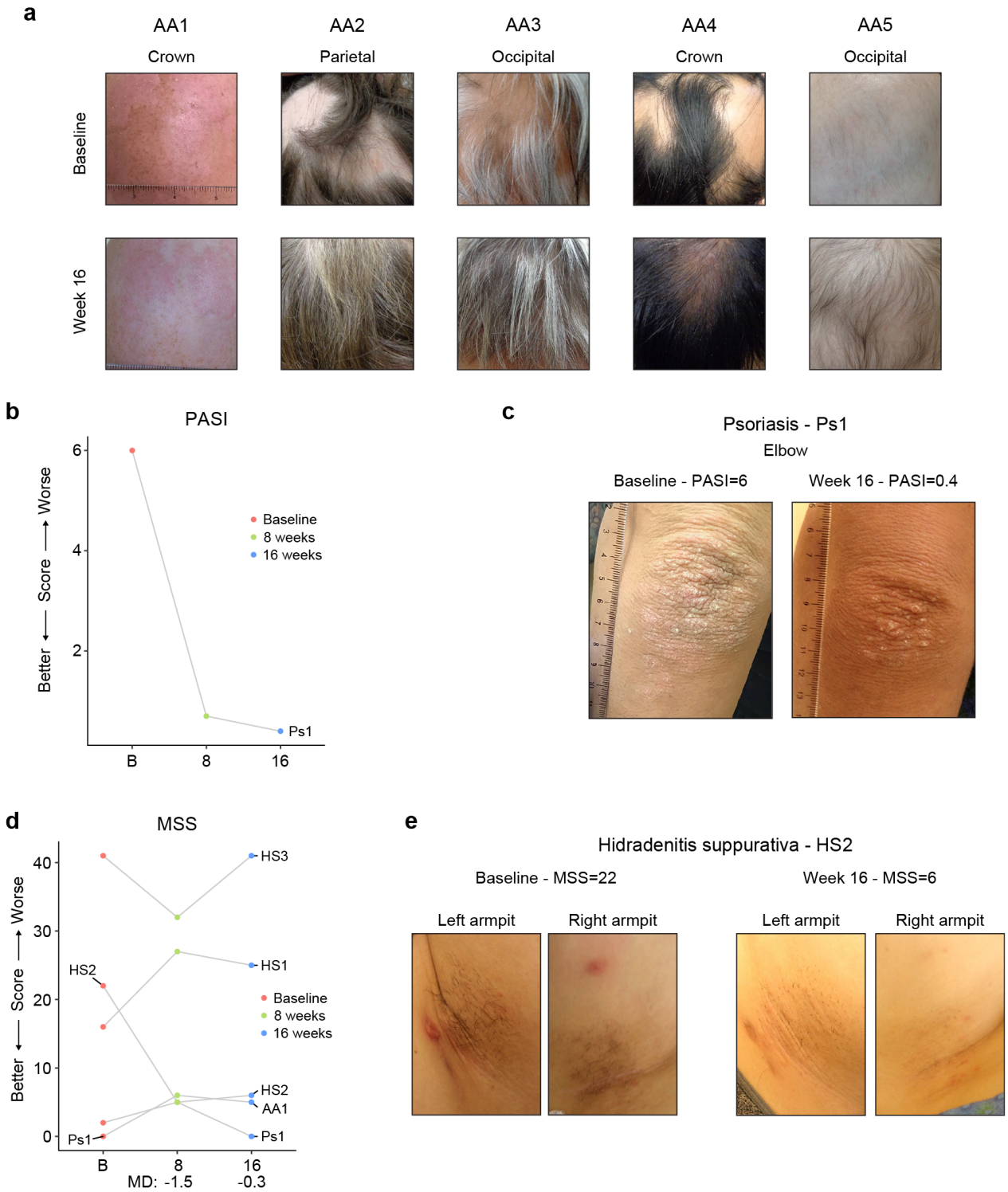

Figure 5 – figure supplement 1. Tofacitinib improves diverse skin pathologies in Down syndrome. **a,** Images of five participants with alopecia areata at baseline and after 16 weeks of tofacitinib treatment. **b-c**, Psoriasis Area and Severity Index score (b) and images (c) for participant with psoriatic arthritis. **d,** Modified Sartorius Scale (MSS) scores for five participants with hidradenitis suppurativa (HS). MD:

448 median difference. **e**, Images for participant affected by HS at baseline and 16-week endpoint visit. p

449 values not shown as per interim analysis plan.

450

451 **Tofacitinib normalizes IFN scores and decreases pathogenic cytokines and autoantibodies.**

452 It is well demonstrated that individuals with DS display elevated IFN signaling across multiple
453 immune and non-immune cell types[15-17,19]. Using an IFN transcriptional score composed of 16 interferon-
454 stimulated genes (ISGs)[55] measured via bulk RNA sequencing of peripheral blood RNA, individuals with
455 DS in the HTP cohort study show a significant increase in these scores[50] (**Figure 6a**). Reduction of IFN
456 scores is designated as a primary endpoint in the trial. At baseline, clinical trial participants show IFN
457 scores within the typical range for DS, but values are decreased at 2, 8, and 16 weeks of tofacitinib
458 treatment (**Figure 6a, Supplementary file 6**). Time course analysis revealed that most participants show
459 a decrease in IFN scores as soon as two weeks of treatment which is sustained over time, with two clear
460 exceptions (**Figure 6 – figure supplement 1a**). At the 8-week study midpoint, 9 of 10 participants had
461 decreased IFN scores relative to baseline, except participant AA2 who reported a COVID-19 vaccination
462 three days prior to the visit and was pausing tofacitinib at the time of the blood draw (**Figure 6 – figure**
463 **supplement 1a**). At the 16-week time point, nine of ten participants had decreased IFN scores, with the
464 exception being AA4, who developed an URI in the week prior to the blood draw (**Figure 6 – figure**
465 **supplement 1a**). Therefore, although all participants displayed decreased IFN scores at one or more time
466 points during the treatment, IFN scores could be sensitive to immune triggers. Analysis of individual ISGs
467 composing the IFN score revealed that whereas many ISGs elevated in DS display reduced expression
468 upon tofacitinib treatment (e.g., *RSAD2*, *IFI44L*), others do not (e.g., *BPGM*) (**Figure 6b, Figure 6 –**
469 **figure supplement 1b**). To investigate this further, we defined the impact of tofacitinib on all 136 ISGs
470 significantly elevated in DS that are not encoded on chr21[44] (**Figure 6c**). Collectively, ISGs as a group
471 are significantly downregulated upon tofacitinib treatment, but the effect is not uniform across all ISGs
472 (**Figure 6c**), indicating that JAK1/3 inhibition does not reduce all IFN signaling elevated in DS, which
473 could be explained by the fact that the IFN pathways also employ JAK2 for signal transduction[56,57]. Global
474 analysis of transcriptome changes revealed that tofacitinib treatment reverses the dysregulation of many
475 gene signatures observed in DS, effectively attenuating many pro-inflammatory signatures beyond IFN

476 gamma and alpha responses, such as Inflammatory Response, TNF-α signaling via NFkB, IL-2 STAT5
477 signaling, and IL-6 JAK STAT3 signaling (**Figure 6 – figure supplement 1c**). Tofacitinib also reversed
478 elevation of genes involved in Oxidative Phosphorylation and dampened downregulation of gene sets
479 involved in Wnt/Beta Catenin and Hedgehog Signaling (**Figure 6 – figure supplement 1c-d**). Conversely,
480 tofacitinib did not rescue elevation of genes involved in Heme Metabolism or Mitotic Spindle (**Figure 6**
481 **– figure supplement 1c-d**), suggesting that these transcriptome changes are not tied to the inflammatory
482 profile of DS.

483 A secondary endpoint in the trial is decrease of peripheral inflammatory markers as defined by a
484 composite cytokine score derived from measurements of TNF-α, IL-6, CRP, and IP-10, and which is
485 significantly increased in participants with DS in the HTP study (**Figure 6d**). At baseline, clinical trial
486 participants show cytokine scores within the range observed for DS, but these values decrease at 2, 8 and
487 16 weeks relative to baseline (**Figure 6d-e, Figure 6 – figure supplement 1e**). The decreases in TNF-α
488 and IL-6 observed upon tofacitinib treatment indicates that elevation of these potent inflammatory
489 cytokines requires sustained JAK/STAT signaling in DS (**Figure 6e**). As for the IFN scores assessment,
490 time course analysis revealed that most participants show decreases in cytokine scores within two weeks
491 of treatment that are sustained over time, again with the exception of AA2 at week 8 and AA4 at week 16.
492 This reveals a correspondence between RNA-based transcriptional IFN scores and circulating levels of
493 these cytokines in plasma, while also illustrating that both metrics may remain sensitive to immune
494 triggers (**Figure 6 – figure supplement 1f-g**).

495 One tertiary endpoint of the trial investigates the impact of tofacitinib treatment on levels of
496 autoantibodies and markers employed to diagnose AITD [e.g., anti-TPO, anti-TG, anti-thyroid stimulating
497 hormone receptor (TSHR)] and celiac disease [e.g., anti-tissue transglutaminase (tTG), anti-deamidated
498 gliadin peptide (DGP)]. Seven of the 10 participants presented at baseline with anti-TPO levels above the
499 upper limit of normal (ULN, 60U/mL), and all seven experienced a decrease in these auto-antibodies at 8
500 weeks and 16 weeks relative to baseline (**Figure 6f**). In fact, for one participant (HS1) the levels decreased

501 below the ULN while on the trial. All seven of these participants had a history of thyroid disease (**Figure**
502 **4c**), which was being medically managed and/or clinically monitored with acceptable TSH and T4 values.
503 Additionally, three of these seven participants also had anti-TG levels above the ULN (4 IU/mL) and all
504 three showed a decrease from baseline levels while on tofacitinib at both 8 and 16 weeks, with one
505 participant (AA6) falling below the ULN upon treatment (**Figure 6f**). Three participants also had anti-
506 TSHr levels above the ULN, but no clear changes were observed upon treatment (**Supplementary file 5**).
507 None of the 10 participants displayed anti-tTG or anti-DGP levels detected above ULN at screening.
508 Altogether, these results indicate that tofacitinib treatment decreases IFN scores, levels of key
509 pathogenic cytokines, and key autoantibodies involved in AITD. Importantly, tofacitinib treatment lowers
510 IFN scores and cytokine levels to within the range observed in the general population, not below,
511 indicating that this immunomodulatory strategy can provide therapeutic benefit in DS without overt
512 immune suppression.
513

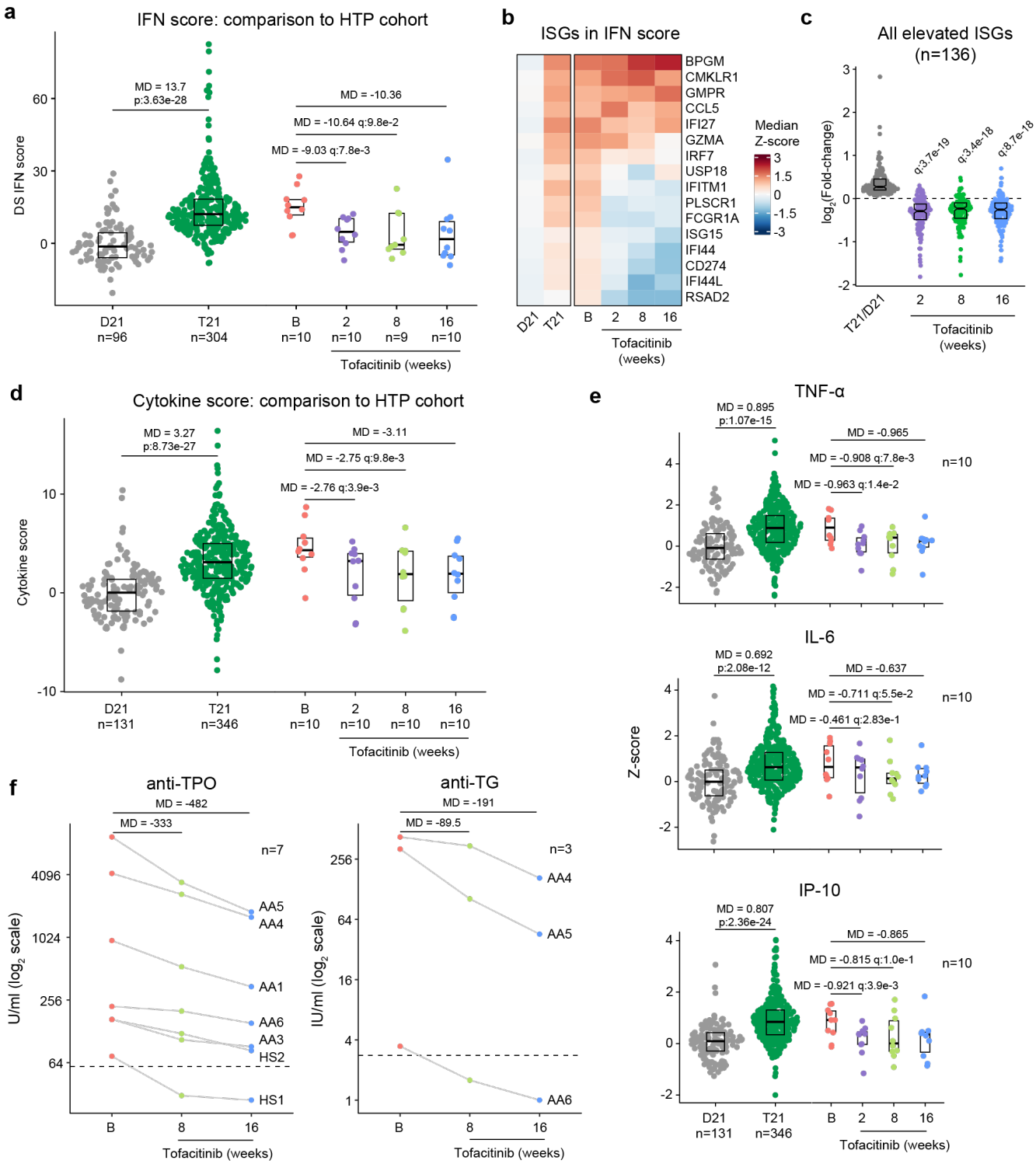

514

515 **Figure 6. Tofacitinib reduces IFN scores, hypercytokinemia, and pathogenic autoantibodies in**
516 **Down syndrome. a,** Comparison of interferon (IFN) transcriptional scores derived from whole blood
517 transcriptome data for research participants in the Human Trisome Project (HTP) cohort study by
518 karyotype status (D21, grey; T21, green) and the clinical trial cohort at baseline (B), and weeks 2, 8 and

519 16 of tofacitinib treatment. Data are represented as modified sina plots with boxes indicating quartiles.
520 Sample sizes are indicated below the x-axis. Horizontal bars indicate comparisons between groups with
521 median differences (MD) with p-values from Mann-Whitney U-tests (HTP cohort) or q-values from paired
522 Wilcox tests (clinical trial). q value for the 16-week endpoint is not shown as per interim analysis plan. **b,**
523 Heatmap displaying median z-scores for the indicated groups (as in a) for the 16 interferon-stimulated
524 genes (ISGs) used to calculate IFN scores. **c,** Analysis of fold changes for 136 ISGs not encoded on chr21
525 that are significantly elevated in Down syndrome (T21 versus D21) at 2, 8 and 16 weeks of tofacitinib
526 treatment relative to baseline. Sample sizes as in a. q-values above each group indicate significance of
527 Mann-Whitney U-tests against log2-transformed fold-change of 0 (no-chance), after Benjamini-Hochberg
528 correction for multiple testing. **d,** Comparison of cytokine score distributions for the HTP cohort by
529 karyotype status (D21, T21) versus the clinical trial cohort at baseline (B) and 2, 8 and 16 weeks of
530 tofacitinib treatment. Data are represented as modified sina plots with boxes indicating quartiles. Sample
531 sizes are indicated below the x-axis. Horizontal bars indicate comparisons between groups with median
532 differences (MD) with p-values from Mann-Whitney U-tests (HTP cohort) and q-values from paired
533 Wilcox tests (clinical trial). q value for the 16-week endpoint is not shown as per interim analysis plan. **e,**
534 Comparison of plasma levels of cytokines in the HTP cohort by karyotype status (D21, T21) and the
535 clinical trial cohort at baseline (B) versus 2, 8 and 16 weeks of tofacitinib treatment. Data are represented
536 as modified sina plots with boxes indicating quartiles. Sample sizes are indicated below x-axis. Horizontal
537 bars indicate comparisons between groups with median differences (MD) with p-values from Mann-
538 Whitney U-tests (HTP cohort) and q values from paired Wilcox tests (clinical trial). q value for the 16-
539 week endpoint is not shown as per interim analysis plan. **f,** Plots showing levels of autoantibodies against
540 thyroid peroxidase (TPO) and thyroglobulin (TG) at baseline versus 8 and 16 weeks of tofacitinib
541 treatment. Sample sizes are indicated in each plot.
542

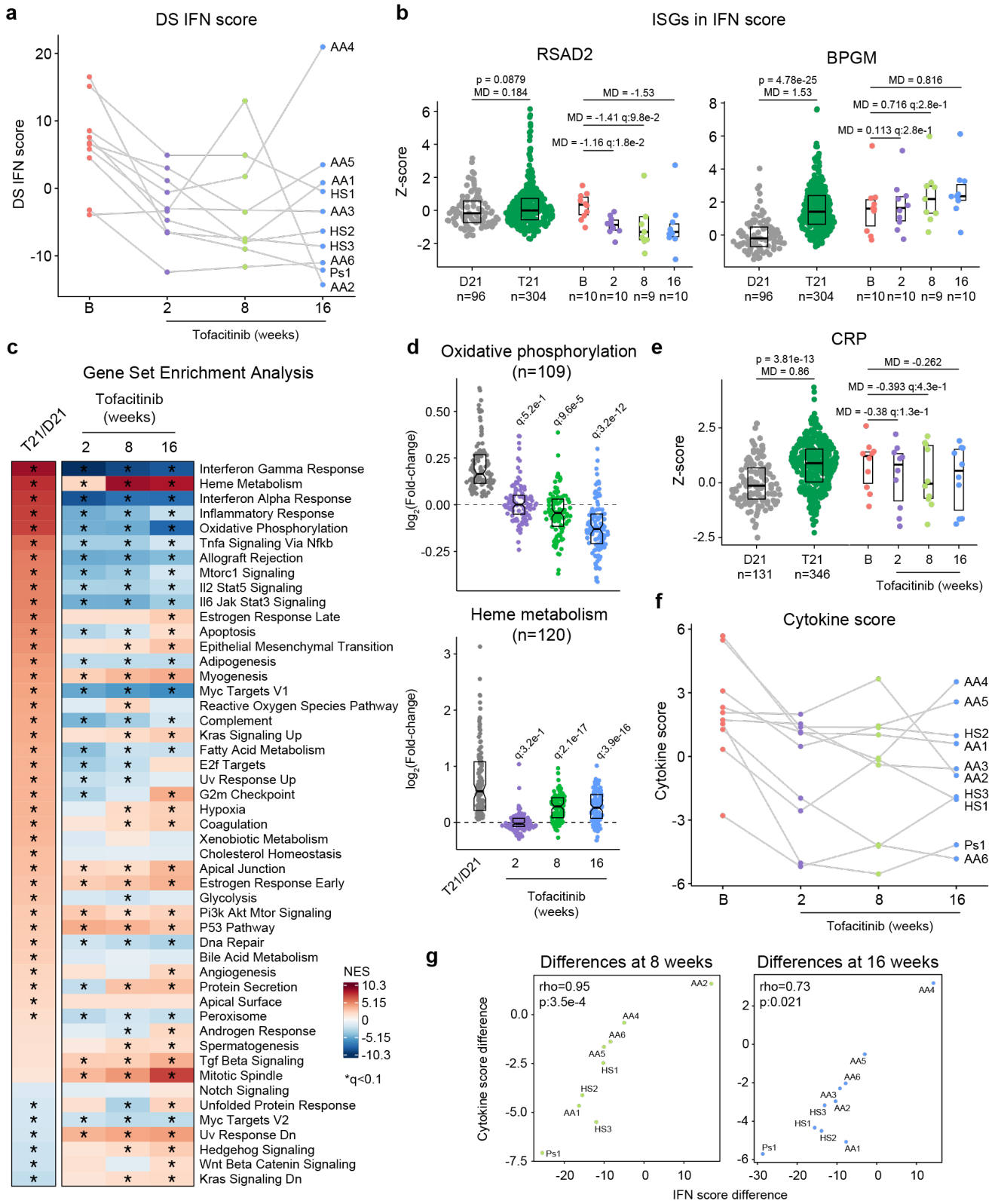

543

544 **Figure 6 – figure supplement 1. JAK inhibition reduces multiple markers of inflammation and**

545 **autoimmunity in Down syndrome. a,** Plot showing trajectory of IFN scores derived from whole blood

546 transcriptome for 10 clinical trial participants at baseline (B), versus 2, 8 and 16 weeks of tofacitinib

547 treatment. **b**, Comparison of ISG expression in the whole blood transcriptome data from research
548 participants in the Human Trisome Project (HTP) cohort study by karyotype status (D21, grey; T21, green)
549 and the clinical trial cohort at baseline (B), and weeks 2, 8 and 16 of tofacitinib treatment. Data are
550 represented as modified sina plots with boxes indicating quartiles. Sample sizes are indicated below x-
551 axis. Horizontal bars indicate comparisons between groups with median differences (MD) with p-values
552 from Mann-Whitney U-tests (HTP cohort) and q-values from paired Wilcox tests (clinical trial). **c,**
553 Heatmap displaying the results of Gene Set Enrichment Analysis (GSEA) of global transcriptome changes
554 in the whole blood RNA of research participants in the HTP cohort (T21, n=304; D21, n=96) versus the
555 clinical trial cohort at 2 (n=10), 8 (n=9), and 16 weeks (n=10) of tofacitinib treatment relative to baseline
556 (n=10). Asterisks indicate significance after correction by Benjamini-Hochberg method for multiple
557 testing (q<0.1, 10% FDR). NES: normalized enrichment score. **d,** Analysis of fold changes for 109 genes
558 involved in oxidative phosphorylation and 120 genes involved in heme metabolism significantly elevated
559 in Down syndrome (T21 versus D21 in the HTP cohort) versus the clinical trial cohort at 2, 8 and 16
560 weeks of tofacitinib treatment relative to baseline. Sample numbers as in c. **e,** Comparison of CRP levels
561 in the HTP cohort by karyotype status (D21, grey; T21, green) versus the clinical trial cohort at baseline
562 (B) and 2, 8 and 16 weeks of tofacitinib treatment. Data are represented as modified sina plots with boxes
563 indicating quartiles. Sample sizes are indicated below x-axis. Horizontal bars indicate comparisons
564 between groups with median differences (MD) with p-values from Mann-Whitney U-tests (HTP cohort)
565 and q-values from paired Wilcox tests (clinical trial). **f,** Plot showing trajectory of cytokine scores for 10
566 clinical trial participants at baseline (B), versus 2, 8 and 16 weeks of tofacitinib treatment. **g,** Plots showing
567 Spearman correlations between fold changes in IFN scores versus cytokine scores at 8 and 16 weeks of
568 tofacitinib treatment versus baseline. Sample size is n=10.
569

570 **Discussion.**

571 An increasing body of evidence indicates that immune dysregulation contributes to the
572 pathophysiology of DS and that immunomodulatory therapies could provide multidimensional benefits in
573 this population. In mouse models, triplication of four *IFNR* genes contributes to multiple hallmarks of
574 DS[50,58] and JAK inhibition attenuates global dysregulation of gene expression[44] while rescuing key
575 phenotypes, such as lethal immune hypersensitivity[22] and CHDs[24]. The fact that gene signatures of IFN
576 hyperactivity are present in human embryonic tissues with T21[59] and embryonic tissues from mouse
577 models of DS[50,60] indicates that the harmful effects of IFN hyperactivity could start *in utero*, supporting
578 the notion that DS could be understood, in part, as an inborn error of immunity with similarities to
579 monogenic interferonopathies[61].

580 Results presented here demonstrate that T21 causes widespread multi-organ autoimmunity of pediatric
581 onset, with production of autoantibodies targeting every major organ system. These results justify
582 additional efforts to define the key pathogenic autoantibodies in DS beyond those commonly associated
583 with AITD and celiac disease. Our analysis found significant associations between specific autoantibodies
584 and some conditions more common in DS, but the diagnostic value of these observations will require
585 validation efforts in much larger cohorts, which could lead to a personalized medicine approach for the
586 management of autoimmunity in DS. For example, we found autoantibodies associated with various forms
587 of auditory dysfunction (**Figure 1g**), suggesting the possibility of autoimmune hearing loss in DS[62].
588 Elevated levels of anti-TPO in individuals with history of use of ear tubes suggests an interplay between
589 otitis media and endocrine dysfunction in DS[63]. For example, it is possible that recurrent ear infections
590 cause a chronic immune stimulus that lead to eventual breach of tolerance in this autoimmunity-prone
591 population, even perhaps through epitope mimicry[64]. Antibodies targeting MUSK, which we found to be
592 elevated in DS and associated with co-occurring neurological phenotypes (**Figure 1g-h**), have been linked
593 to development of myasthenia gravis, a chronic autoimmune neuromuscular disease that causes weakness
594 in the skeletal muscles[65]. Whether MUSK antibodies associate with similar phenotypes in DS will require

595 further investigation. Elevation of SRP68 autoantibodies in DS (**Figure 1d,f**), which are common in
596 necrotizing myopathies with cardiovascular involvement[42], suggests a potential autoimmune basis for
597 musculoskeletal and cardiovascular complications in DS, which also warrants additional research.

598 We observed constitutive global immune remodeling and hypercytokinemia regardless of reported
599 diagnoses of autoimmune disease or measurable autoantibody production from an early age, indicative of
600 an autoimmunity-prone state throughout the lifespan. Although many cytokines elevated in DS have well
601 demonstrated pathogenic roles in the etiology of autoimmune diseases in the general population (e.g.,
602 TNF-α, IL6), their consistent upregulation in DS regardless of clinical evidence of autoimmune pathology
603 indicates the existence of a prolonged pre-clinical period, where the hypercytokinemia likely precedes
604 evident tissue damage and symptomology. Alternatively, it is possible that these elevated cytokines are
605 contributing the overall pathophysiology of DS (e.g., cognitive impairments, complications from viral
606 infections) without formal diagnosis of an autoimmune disease. Therefore, measurements of specific
607 immune cell types or cytokines in the bloodstream are unlikely to provide diagnostic value for
608 autoimmunity in DS. However, antigen-specific immune assays, such as T cell or B cell activation assays,
609 may reveal the specific timing of loss of tolerance and transition to clinical phenotypes. Future studies
610 should also include analysis of tissue-resident immune cells, which may identify sites of local autoimmune
611 attack in DS.

612 Among the many strategies that could be used to attenuate IFN hyperactivity, JAK inhibitors are the
613 most well-studied and have the most approved indications[66]. Of the more than ten globally-approved JAK
614 inhibitors[66], we chose to employ in our clinical trial the JAK1/3 inhibitor tofacitinib, which is used to treat
615 diverse autoimmune/inflammatory conditions and which was approved in 2020 for treatment of
616 polyarticular course juvenile idiopathic arthritis (pcJIA) in children 2 years and older[66,67]. Notably, all four
617 IFNRs encoded on chr21 utilize JAK1 for signal transduction in combination with either JAK2 or TYK2,
618 making JAK1 inhibitors the most logical choice to dampen the effects of *IFNR* gene triplication. As part
619 of the clinical trial protocol, the approved interim analysis was designed to qualitatively evaluate

620 feasibility and initial safety data on the first 10 participants completing a 16-week course of tofacitinib
621 treatment. This analysis established that there were no AEs that required a change or cessation of
622 tofacitinib dosing and that this medicine is well tolerated in individuals with DS. The clear benefits
623 observed for diverse autoimmune skin conditions align with an increasing body of evidence supporting
624 the use of JAK inhibition for immunodermatological conditions, including their recent approval for
625 alopecia areata and atopic dermatitis in the general population[68,69]. At this sample size, the effects of
626 tofacitinib on HS are inconclusive. Although some participants and caregivers reported benefits in terms
627 of fewer flares of lesser severity, the MSS metric did not show a clear trend, which may reveal the need
628 for more frequent or different types of monitoring for HS, a condition that cycles periodically in severity.
629 Our results indicate that tofacitinib does not fully suppress the immune response in people with DS,
630 but rather attenuates IFN scores and cytokine scores to levels observed in the general population, which
631 is an important consideration given the likely requirement for long-term use of the drug in this population.
632 Furthermore, the effects of the drug are clearly gene-specific, highlighting the presence of inflammatory
633 processes that may not be attenuated with this inhibitor, which could be beneficial in terms of preserving
634 immune activity. Importantly, during treatment, both IFN scores and cytokine scores remain sensitive to
635 immune stimuli, as evidenced by participants who had received a vaccine or experienced an URI before a
636 blood draw (**Figure 6a**, **Figure 6 – figure supplement 1f**). Overall, it is encouraging that key
637 inflammatory markers decreased in a relatively short timeframe, likely offering systemic benefits beyond
638 skin pathology. Importantly, the fact that levels of IL-6 and TNF-α are reduced upon tofacitinib treatment
639 supports the use of JAK inhibitors over TNF-blockers or anti-IL-6 agents in this population. Although
640 TNF-α-blockers are recommended to be used first in the treatment of rheumatoid arthritis in the general
641 population[70], the value of this recommendation in people with DS remains to be defined. The clear
642 decrease in anti-TPO and anti-TG levels indicates that autoreactive B cell function requires elevated
643 JAK/STAT signaling, but whether this effect is cell-autonomous versus a consequence of a reduced
644 systemic inflammatory milieu will require further investigation. Defining the effect of tofacitinib on other

645 autoantibodies elevated in DS will also require a larger sample size and may be revealed in the full dataset
646 after completion of this trial, along with analysis of potential remodeling of the B cell lineage upon JAK
647 inhibition, such as effects on mature B cells and plasmablast populations.

648 Lastly, this ongoing clinical trial includes measurements of various dimensions of neurological
649 function not reported here. Although the absence of a placebo control arm may impede a clear
650 interpretation of any effect of JAK inhibition on cognitive function, preliminary results have prompted
651 the design and launch of a second trial (NCT05662228) aimed at defining the relative safety and efficacy
652 of tofacitinib, intravenous immunoglobulin (IVIG), and the benzodiazepine lorazepam for Down
653 syndrome Regression Disorder (DSRD), a condition characterized by sudden loss of neurological
654 function[71].

655 Altogether, these findings justify both a deeper investigation of all the deleterious effects of
656 autoimmunity and hyperinflammation in DS and the expanded testing of immunomodulatory strategies
657 for diverse aspects of DS pathophysiology, even perhaps from an early age.

658

659 **Materials and Methods.**

660 **Human Trisome Project (HTP) study.**

661 All aspects of this study were conducted in accordance with the Declaration of Helsinki under protocols
662 approved by the Colorado Multiple Institutional Review Board. Results and analyses presented herein are
663 part of a nested study within the Crnic Institute's Human Trisome Project (HTP, NCT02864108, see also
664 www.trisome.org) cohort study. All study participants, or their guardian/legally authorized representative,
665 provided written informed consent. The HTP study has generated multiple multi-omics datasets on
666 hundreds of research participants, some of which have been analyzed in previous studies, including whole
667 blood transcriptome data[44], white blood cell transcriptome data[19], plasma proteomics[44], plasma
668 metabolomics[19,44], and immune mapping via flow cytometry[16] and mass cytometry[44,50]. This paper reports
669 new analyses of select previous datasets (transcriptome, mass cytometry, MSD immune markers) within
670 the larger multi-omics dataset of the HTP study, as well as analyses of new datasets (e.g., anti-TPO, ANA,
671 autoantibodies), as described in detail below.

672 **Annotation of co-occurring conditions.**

673 Within the HTP, a clinical history for each participant is curated from both medical records and
674 participant/family reports. Both surveys are set up as REDCap[72] instruments that collect information as a
675 review of systems (e.g., cardiovascular, immunity, endocrine). Expert data curators complete the medical
676 record review and evaluate answers provided by self-advocates and caregivers. In cases of discordant
677 answers across the two instruments, medical records take precedence. De-identified demographic and
678 clinical metadata obtained is then linked to de-identified biospecimens used to generate the various -omics
679 (e.g., RNA sequencing) and targeted assay datasets (e.g., anti-TPO assays). For annotation of AITD,
680 several possible entries were considered as shown in **Figure 1 – figure supplement 1a**, including history
681 of hypothyroidism, hyperthyroidism, Hashimoto's disease, Grave's disease, anti-TPO or -TG antibodies,
682 and subclinical hypothyroidism. For annotation of immune skin conditions, atopic dermatitis and eczema

683 were combined and counted in a single group, as were hidradenitis suppurativa (HS), folliculitis, and
684 'boils'.

685 **Blood sample collection and processing.**

686 The biological datasets analyzed herein were derived from peripheral blood samples collected using
687 PAXgene RNA Tubes (Qiagen) and BD Vacutainer K2 EDTA tubes (BD). Whole blood from PAXgene
688 collection tubes was processed for RNA sequencing as described below. Two 0.5 mL aliquots of whole
689 blood were withdrawn from each EDTA tube and processed for mass cytometry as described below. The
690 remaining EDTA blood samples were centrifuged at 700 x g for 15 min to separate plasma, buffy coat
691 containing white blood cells (WBC), and red blood cells (RBCs). Samples were then aliquoted, flash
692 frozen and stored at -80°C until subsequent processing and analysis. Centrifugation and storage of samples
693 took place within 2 hours of collection.

694 **Measurements of autoantibodies.**

695 Anti-TPO status was determined from plasma samples using an electrochemiluminescence-based assay
696 [73], and carried out by the Autoantibody/HLA Core Facility of the Barbara Davis Center for Childhood
697 Diabetes at the University of Colorado Anschutz Medical Campus. Sample values were calculated as
698 (sample signal – negative control signal) / (positive control signal – negative control signal), with the
699 threshold (upper limit of normal) for TPO positivity based on the 95th percentile of healthy control
700 samples.

701 Anti-nuclear antigen (ANA) status was determined from plasma samples using a qualitative ELISA kit
702 (MyBioSource, cat. no. 702970) according to manufacturer instructions, with a sample OD_{450nm} / negative
703 control OD_{450nm} ratio ≥ 2.1 evaluated as positive and a ratio < 2.1 evaluated as negative.

704 Autoantigen profiling of EDTA plasma samples (50 µL each; T21, n = 120; D21, n = 60) was performed
705 by the Affinity Proteomics unit at SciLifeLab (KTH Royal Institute of Technology, Stockholm, Sweden)
706 using peptide arrays. Antigens were selected to cover potential associations to autoimmune diseases and
707 consisted of 380 peptide fragments covering ~270 unique proteins (1-5 fragments per protein). Fragments

708 were ~20-163 amino acids long (median 82). All antigens were expressed in E. coli with a hexahistidyl
709 and albumin binding protein tag (His6ABP). Using, COOH-NH2 chemistry, the analyzed antigens, in
710 addition to controls, were immobilized on color-coded magnetic beads (MagPlex, Luminex). Controls
711 consisted of His6ABP, buffer, rabbit anti-human IgG (loading control, Jackson ImmunoResearch), and
712 Epstein-Barr nuclear antigen 1 (EBNA1, Abcam). Research samples and technical controls (commercial
713 plasma; Seralab) were diluted (1:250) in assay buffer, which consisted of 3% BSA, 5% milk, 0.05%
714 Tween-20, and 160 μg/ml His6ABP tag in PBS. Diluted samples and controls were incubated for 1 hour
715 at room temperature then subsequently incubated with the antigen bead array for 2 hour. The reactions
716 were then fixed for 10 minutes using 0.02% paraformaldehyde, then incubated for 30 minutes with goat
717 Fab specific for human IgG Fc-γ tagged with the fluorescent marker R-phycoerythrin (Invitrogen). Median
718 fluorescence intensity (MFI) and number of beads for each reaction was analyzed using a FlexMap 3D
719 instrument (Luminex Corp.). Quality control was performed using MFI and bead count to exclude antigens
720 and samples not passing technical criteria including minimal bead counts and antigen coupling efficiency.
721 To adjust for sample specific backgrounds, MFI values were transformed per reaction median absolute
722 deviations (MADs) using the following calculation:

723 $$MADs_{sample} = (MFI - median_{sample(MFI)}) / MAD_{sample(MFI)}$$

724 Subsequent data analysis and handling was performed using R. For each antigen, positivity was defined
725 as >90th percentile MAD value for D21 samples only. Overrepresentation of positivity for each antigen
726 in the T21 versus D21 group was determined using Fisher's exact test, excluding antigens detected in <18
727 samples (<10% of total experiment). Correction for multiple testing was performed using the Benjamini-
728 Hochberg approach and significance defined as q<0.1 (10% FDR). Similarly, within the T21 group,
729 Fisher's exact test was used to test for overrepresentation of antigen positivity in cases versus controls for
730 co-occurring conditions, with only those with at least 5 cases considered in the analysis.

731 **Immune profiling via mass cytometry.**

732 Generation of the mass cytometry dataset was described previously[44], but a full description is included
733 here for reference. Two 0.5 mL aliquots of EDTA whole blood samples underwent RBC lysis and white
734 blood cell fixation using TFP FixPerm Buffer (Transcription Factor Phospho Buffer Set, BD Biosciences).
735 WBCs were then washed in 1x in PBS (Rockland), resuspended in Cell Staining Buffer (Fluidigm) and
736 stored at −80°C. For antibody staining, samples were thawed at room temperature, washed in Cell Staining
737 Buffer, barcoded using a Cell-ID 20-Plex Pd Barcoding Kit (Fluidigm), and combined per batch. Each
738 batch was able to accommodate 19 samples with a common reference sample. Antibodies were either
739 purchased pre-conjugated to metal isotopes or conjugation was performed in-house using a Maxpar
740 Antibody Labeling Kit (Fluidigm). See **Supplementary file 7** for antibodies. Working dilutions for
741 antibody staining were titrated and validated using the common reference sample and comparison to
742 relative frequencies obtained by independent flow cytometry analysis. Surface marker staining was carried
743 out for 30 min at 4°C in Cell Staining Buffer with added Fc Receptor Binding Inhibitor
744 (eBioscience/ThermoFisher Scientific). Staining was followed by a wash in Cell Staining Buffer. Next,
745 cells were permeabilized in Buffer III (Transcription Factor Phospho Buffer Set, BD Pharmingen) for 20
746 min at 4°C followed by washing with perm/wash buffer (Transcription Factor Phospho Buffer Set, BD
747 Pharmingen). Intracellular transcription factor and phospho-epitope staining was carried out for 1 hour at
748 4°C in perm/wash buffer (Transcription Factor Phospho Buffer Set, BD Pharmingen), followed by a wash
749 with Cell Staining Buffer. Cell-ID Intercalator-Ir (Fluidigm) was used to label barcoded and stained cells.
750 Labeled cells were analyzed on a Helios instrument (Fluidigm). Mass cytometry data were exported as
751 v3.0 FCS files for pre-processing and analysis.

752 *Analysis of mass cytometry data.*

753 *Pre-processing.* Bead-based normalization via polystyrene beads embedded with lanthanides, both within
754 and between batches, followed by bead removal was carried out as previously described using the Matlab-
755 based Normalizer tool[74]. Batched FCS files were demultiplexed using the Matlab-based Single Cell
756 Debarcoder tool[75]. Reference-based normalization of individual samples across batches against the

757 common reference sample was then carried out using the R script *BatchAdjust()*. For the analyses
758 described in this manuscript, CellEngine (CellCarta) was used to gate and export per-sample FCS files at
759 four levels: Firstly, CD3+CD19+ doublets were excluded and remaining cells exported as 'Live' cells;
760 Live cells were then gated for hematopoietic lineage (CD45-positive) non-granulocytic (CD66-low) cells
761 and exported as CD45+CD66low. Lastly, CD45+CD66low cells were gated on CD3-positivity and CD19-
762 positivity and exported as T- and B-cells, respectively. Per-sample FCS files were then subsampled to a
763 maximum of 50,000 events per file for subsequent analysis.
764 *Unsupervised clustering.* For each of the four levels (live, non-granulocytes, T cells, and B cells), all 388
765 per-sample FCS files were imported into R as a flowSet object using the *read.flowSet()* function from the
766 flowCore R package[76]. Next a SingleCellExperiment object was constructed from the flowSet object using
767 the *prepData()* function from the CATALYST package[77]. Arcsinh transformation was applied to marker
768 expression data with cofactor values ranging from ~0.2 to ~15 to give optimal separation of positive and
769 negative populations for each marker, using the *estParamFlowVS()* function from the flowVS R package[78]
770 and based on visual inspection of marker histograms (see **Supplementary file 7)**. Quality control and
771 diagnostic plots were examined with the help of functions from CATALYST and the
772 tidySingleCellExperiment R package. Unsupervised clustering using the FlowSOM algorithm[45] was
773 carried out using the *cluster()* function from CATALYST, with grid size set to 10 x 10 to give 100 initial
774 clusters and a maxK value of 40 was explored for subsequent meta-clustering using the
775 ConsensusClusterPlus algorithm. Examination of delta area and minimal spanning tree plots indicated that
776 30-40 meta clusters gave a reasonable compromise between gains in cluster stability and number of
777 clusters for each level. Each clustering level was re-run with multiple random seed values to ensure
778 consistent results.
779 *Visualization using t-distributed stochastic neighbor imbedding (tSNE).* Dimensionality reduction to two
780 dimensions was carried out using the *runDR()* function from the CATALYST package, with 500 cells per
781 sample, and using several random seed values to ensure consistent results. Multiple values of the

782 perplexity parameter were tested, with a setting of 440, using the formula Perplexity=N^(1/2) as suggested
783 at https://towardsdatascience.com/how-to-tune-hyperparameters-of-tsne-7c0596a18868, providing a
784 visualization with good agreement with the clusters defined by FlowSOM.
785 *Cell type classification.* To aid in assignment of clusters to specific lineages and cell types, the MEM
786 package (marker enrichment modeling) was used to call positive and negative markers for each cell cluster
787 based on marker expression distributions across clusters. Manual review and comparison to marker
788 expression histograms, as well as minimal spanning tree plots and tSNE plots colored by marker
789 expression, allowed for high-confidence assignment of most clusters to specific cell types. Clusters that
790 were insufficiently distinguishable were merged into their nearest cluster based on the minimal spanning
791 tree. Relative frequencies for each cell type / cluster were calculated for each sample as a percentage of
792 total live cells and as a percentage of cells used for each level of clustering: total CD45+CD66low cells,
793 total T cells, or total B cells.
794 *Beta regression analysis.* To identify cell clusters for which relative frequencies are associated with either
795 trisomy 21 status or with various clinical subgroups (e.g. ANA+) among individuals with trisomy 21, beta
796 regression analysis was carried out using the betareg R package, with each model using cell type cluster
797 proportions (relative frequency) as the outcome/dependent variable and either T21 status or clinical
798 subgroups as independent/predictor variables, along with adjustment for age and sex, and a logit link
799 function. Extreme outliers were classified per-karyotype and per-cluster as measurements more than three
800 times the interquartile range below or above the first and third quartiles, respectively (below Q1 - 3*IQR
801 or above Q3 + 3*IQR) and excluded from beta regression analysis. Correction for multiple comparisons
802 was performed using the Benjamini-Hochberg (FDR) approach. Effect sizes (as fold-change in T21 vs.
803 euploid controls or among T21 subgroups) for each cell type cluster were obtained by exponentiation of
804 beta regression model coefficients. Fold-changes were visualized by overlaying on tSNE plots using
805 ggplot2. For visualization of individual clusters, data points were adjusted for age and sex, using the

806 *adjust()* function from the datawizard R package, and visualized as sina plots (separated by T21 status or
807 clinical subgroup).

808 **Measurement of immune markers and calculation of cytokine scores.**

809 Briefly, from each EDTA plasma sample, two replicates of 12-25 μL were analyzed using the Meso Scale
810 Discovery (MSD) multiplex immunoassay platform V-PLEX Human Biomarker 54-Plex Kit (HTP
811 cohort) or U-PLEX Human Biomarker Group 1 71-Plex and V-PLEX Human Vascular Injury Panel 2
812 Kits (clinical trial cohort) on a MESO QuickPlex SQ 120 instrument. Assays were carried out as per
813 manufacturer instructions. Concentration values were calculated against a standard curve with provided
814 calibrators. MSD data are reported as concentration values in picograms per milliliter of plasma.

815 *Analysis of immune marker data.* Plasma concentration values (pg/mL) for each of the cytokines and
816 related immune factors measured across multiple MSD assay plates was imported to R, combined, and
817 analytes with >10% of values outside of detection or fit curve range flagged. For each analyte, missing
818 values were replaced with either the minimum (if below fit curve range) or maximum (if above fit curve
819 range) calculated concentration per plate/batch and means of duplicate wells used for subsequent analysis.
820 For the HTP study analysis, extreme outliers were classified per-karyotype and per-analyte as
821 measurements more than three times the interquartile range below or above the first and third quartiles,
822 respectively, and excluded from further analysis. Differential abundance analysis for inflammatory
823 markers measured by MSD was performed using mixed effects linear regression as implemented in the
824 *lmer()* function from the lmerTest R package (v3.1-2) with log2-transformed concentration as the
825 outcome/dependent variable, T21 status or clinical subgroup (e.g., ANA+) as the predictor/independent
826 variable, age and sex as fixed covariates, and sample source as a random effect. Multiple hypothesis
827 correction was performed with the Benjamini-Hochberg method using a false discovery rate (FDR)
828 threshold of 10% ($q < 0.1$). Prior to visualization or correlation analysis, MSD data were adjusted for age,
829 sex, and sample source using the *removeBatchEffect()* function from the limma package (v3.44.3).

830 *Calculation of cytokine scores.* For comparison of clinical trial samples across time points, cytokine scores
831 were calculated as the sum of the Z-scores for TNF-α, IL-6, CRP and IP-10. For comparison of clinical
832 trial samples to the HTP cohort, Z-scores were first calculated from age-, sex, and batch-adjusted values
833 for each sample, based on the mean and standard deviation of the HTP euploid control samples.

834 **Whole blood transcriptome analysis and calculation of IFN scores.**

835 Strand-specific sequencing libraries were prepared from globin-depleted, polyA-enriched whole blood
836 RNA and sequenced on the Illumina NovaSeq platform (2x 150 bases). Data quality was assessed using
837 FASTQC (v0.11.5) and FastQ Screen (v0.11.0). Trimming and filtering of low-quality reads was
838 performed using bbduk from BBTools (v37.99) and fastq-mcf from ea-utils (v1.05). Alignment to the
839 human reference genome (GRCh38) was carried out using HISAT2 (v2.1.0) in paired, spliced-alignment
840 mode against a GRCh38 index and Gencode v33 basic annotation GTF, and alignments were sorted and
841 filtered for mapping quality (MAPQ > 10) using Samtools (v1.5). Gene-level count data were quantified
842 using HTSeq-count (v0.6.1) with the following options (--stranded=reverse –minaqual=10 –type=exon --
843 mode=intersection-nonempty) using a Gencode v33 GTF annotation file. Differential gene expression in
844 T21 versus D21 was evaluated using DESeq2 (version 1.28.1)[79], with $q < 0.1$ (10% FDR) as the threshold
845 for differential expression.

846 *DS IFN scores.* RNA-seq-based 'Down syndrome interferon scores' (DS IFN scores) were calculated as
847 follows: for comparison of clinical trial samples across time points, DS IFN scores were calculated as the
848 sum of Z-scores across 16 interferon-stimulated genes (ISGs) genes with significant mean fold-change of
849 at least 1.5 in the HTP T21 group vs. the euploid control group, excluding *IFNAR2*, *MX1*, and *MX2* which
850 are encoded on chromosome 21. For comparison of clinical trial samples to the HTP cohort, gene-wise Z-
851 scores were first calculated from age-, sex, and sequencing batch-adjusted FPKM values for each sample,
852 based on the mean and standard deviation of the HTP euploid control samples.

853 *Gene set enrichment analysis (GSEA).* GSEA[80] was carried out in R using the fgsea package (v1.14.0),
854 using Hallmark gene sets, log_2-transformed fold-change values as the ranking metric.

855 **Clinical trial design and oversight.**

856 All aspects of this study were conducted in accordance with the Declaration of Helsinki. All study
857 activities were approved by the Colorado Multiple Institutional Review Board (COMIRB, protocol # 19-
858 1362, NCT04246372) with an independent Data and Safety Monitoring Board (DSMB) appointed by the
859 National Institute of Arthritis and Musculoskeletal and Skin Diseases (NIAMS). Written consent was
860 obtained from all participants, or their legally authorized representative if the participant was unable to
861 provide consent, in which case participant assent was obtained. The Clinical Trial Protocol is provided in
862 the **Supplementary file 8**. We report here interim results of a single-site, open-label phase 2 clinical trial
863 enrolling individuals with DS between the ages of 12 and 50 years old with moderate-to-severe alopecia
864 areata, hidradenitis suppurativa, psoriasis, atopic dermatitis, or vitiligo. Qualifying disease scores are
865 shown in **Supplementary file 3**. After screening, qualifying participants are prescribed 5 mg tofacitinib
866 twice daily for 16 weeks, with an optional extension arm to week 40. During the main 16-week trial,
867 participants attend five safety monitoring visits after enrollment at the Baseline visit.

868 **Trial Population.**

869 The recruitment goal for this trial is 40 participants completing 16 weeks of tofacitinib treatment, with a
870 qualitative interim analysis triggered when 10 participants completed the main 16-week trial. Of the 10
871 participants included in the interim analysis, 4 are female, 100% identify as White/Caucasian, 3 identify
872 as Hispanic or Latino, and mean age at enrollment was 23.1 years old (range 15-38.1 years old)
873 (**Supplementary file 3**). Baseline qualifying conditions of the 10 participants were alopecia areata: n=6
874 (46.1%), hidradenitis suppurativa: n=3 (30.8%), or psoriasis: n=1 (7.7%). Two participants also had atopic
875 dermatitis, and two others had vitiligo, albeit below the severity required to be the qualifying condition.

876 **Outcome Measures.**

877 *Primary endpoints.* The two primary outcome measures for this trial are safety and reduction in IFN
878 transcriptional scores derived from peripheral whole blood. Based on the safety profile for tofacitinib in
879 the general population[70], the safety primary endpoint was defined as no more than two serious adverse
880 events (SAEs) definitely attributable to tofacitinib over the course of 16 weeks for 40 participants. Adverse
881 events were classified based using Common Terminology Criteria for Adverse Events 5.0 (CTCAE 5.0).
882 IFN scores are commonly used to monitor disease severity and response to treatment in IFN-driven
883 pathologies[81,82] and their calculation form RNAseq data is described above.
884 *Secondary endpoints.* The secondary outcome measures for this trial include improvements in skin health
885 as defined by a global assessment, the Investigator Global Assessment (IGA), as well as the disease-
886 specific assessments. Overall skin pathology, accounting for all present skin conditions regardless of
887 severity, was assessed using a modified IGA which scores on a five-point scale for each skin condition
888 (six points for HS) with a range of 0-21. Another secondary endpoint assessing global skin health is a
889 change in the Dermatological Quality of Life Index (DLQI), used to assess participant-reported impact of
890 skin conditions on self-image, relationships, and daily activities. Possible total scores range from 0-30,
891 with higher scores indicating a more impaired quality of life. Condition-specific assessments used are
892 Severity of Alopecia Tool (SALT) for AA affecting at least 25% of the scalp (qualifying score is ≥ 25);
893 Hidradenitis Suppurativa-Physicians Global Assessment (HS-PGA) to define eligibility (qualifying score
894 ≥3) and Modified Sartorius Scale (MSS) to monitor changes throughout the study for HS; Psoriasis Area
895 and Severity Index (PASI, qualifying score is ≥10) for psoriasis; Vitiligo Extent Tensity Index (VETI,
896 qualifying score is ≥2), for moderate-to-severe vitiligo; and Eczema Area and Severity Index (EASI,
897 qualifying EASI score ≥16) for moderate-to-severe atopic dermatitis. The last secondary endpoint is
898 reduction in a cytokine score coalescing information on four inflammatory markers elevated in DS: Tumor
899 Necrosis Factor Alpha (TNF-α), interleukin 6 (IL-6), C-reactive protein (CRP), and IFN-inducible protein
900 10 (IP10, CXCL10)[18]. Measurement of these proteins and calculation of the cytokine score is described
901 above.

902 *Tertiary endpoints.* This clinical trial includes multiple exploratory tertiary endpoints (see full protocol in
903 **Supplementary file 8**), including reduction in autoantibodies related to AITD (anti-TPO, anti-TG, and
904 anti-TSHr) and celiac disease (anti-tTG, anti-DGP) . In the clinical trial, these autoantibodies were
905 assessed using established clinical assays.

906 **Statistical Analysis.**

907 The Statistical Analysis Plan (SAP) approved by the appointed DSMB is included with the Clinical Trial
908 Protocol in the **Supplementary file 8**. This report includes analysis of the time points used to assess
909 endpoints (baseline and 16 weeks), as well research-only time points at 2 and 8 weeks of treatment. Given
910 the qualitative nature of this interim analysis, statistical analysis is not completed for changes observed
911 between baseline and the 16-week endpoint. Data may be displayed as $\log_2$ transformed for clarity in
912 viewing the graphs.

913

914 **Data Availability Statement:**

915 A collection with datasets used in this study is available in Synapse
916 (https://doi.org/10.7303/syn53185135), with the individual datasets also accessible as detailed below.
917 Demographic and health history data for research participants in the HTP study are available on both the
918 Synapse data sharing platform (https://doi.org/10.7303/syn31488784) and through the INCLUDE Data
919 Hub (https://portal.includedcc.org/). Mass cytometry data for 380+ HTP research participants are
920 available both in Synapse (https://doi.org/10.7303/syn53185253) and FlowRepository, Study ID FR-
921 FCM-Z5GE,
922 https://flowrepository.org/id/RvFrQaBqhe8TGyko1OMdQKtR7HN8nulAnHW0PJkm1CEyyo8fnJg2rHr
923 WvNrhE8xu. Targeted plasma proteomics for inflammatory markers using Meso Scale Discovery (MSD)
924 assays for 470+ HTP research participants can be accessed through Synapse
925 (https://doi.org/10.7303/syn31475487) and the INCLUDE Data Hub. Whole blood transcriptome data for
926 400 HTP research participants can be accessed through Synapse (https://doi.org/10.7303/syn31488780),

927 the INCLUDE Data Hub, and NCBI Gene Expression Omnibus (GSE190125). Whole blood
928 transcriptome data for 10 clinical trial participants at baseline and after 2, 8, and 16 weeks of tofacitinib
929 treatment can be accessed through Synapse (https://doi.org/10.7303/syn53185250), and NCBI Gene
930 Expression Omnibus (GSE PENDING). Targeted plasma proteomics for inflammatory markers using
931 Meso Scale Discovery (MSD) assays for 10 clinical trial participants can be accessed through Synapse
932 (https://doi.org/10.7303/syn53185252).

933

934 **Code Availability Statement:** No custom code or algorithms were developed during the course of this
935 study. R analysis scripts will be made available upon request.

936

937 **References.**

938 1 Lejeune, J., Turpin, R. & Gautier, M. [Mongolism; a chromosomal disease (trisomy)]. *Bull Acad*
939 *Natl Med* **143**, 256-265 (1959).

940 2 Antonarakis, S. E. *et al.* Down syndrome. *Nature reviews. Disease primers* **6**, 9 (2020).
941 https://doi.org:10.1038/s41572-019-0143-7

942 3 Chicoine, B. *et al.* Prevalence of Common Disease Conditions in a Large Cohort of Individuals
943 With Down Syndrome in the United States. *J Patient Cent Res Rev* **8**, 86-97 (2021).
944 https://doi.org:10.17294/2330-0698.1824

945 4 Amr, N. H. Thyroid Disorders in Subjects with Down Syndrome: An Update. *Acta Biomed* **89**,
946 132-139 (2018). https://doi.org:10.23750/abm.v89i1.7120

947 5 Pierce, M. J., LaFranchi, S. H. & Pinter, J. D. Characterization of Thyroid Abnormalities in a
948 Large Cohort of Children with Down Syndrome. *Hormone research in paediatrics* **87**, 170-178
949 (2017). https://doi.org:10.1159/000457952

950 6 Iughetti, L. *et al.* Ten-year longitudinal study of thyroid function in children with Down's
951 syndrome. *Hormone research in paediatrics* **82**, 113-121 (2014).
952 https://doi.org:10.1159/000362450

953 7 Book, L. *et al.* Prevalence and clinical characteristics of celiac disease in Downs syndrome in a
954 US study. *American journal of medical genetics* **98**, 70-74 (2001).

955 8 Zachor, D. A., Mroczek-Musulman, E. & Brown, P. Prevalence of celiac disease in Down
956 syndrome in the United States. *Journal of pediatric gastroenterology and nutrition* **31**, 275-279
957 (2000).

958 9 Sureshbabu, R. *et al.* Phenotypic and dermatological manifestations in Down Syndrome.
959 *Dermatology online journal* **17**, 3 (2011).

960 10 Madan, V., Williams, J. & Lear, J. T. Dermatological manifestations of Down's syndrome.
961 *Clinical and experimental dermatology* **31**, 623-629 (2006). https://doi.org:10.1111/j.1365-
962 2230.2006.02164.x
963 11 Lam, M., Lai, C., Almuhanna, N. & Alhusayen, R. Hidradenitis suppurativa and Down
964 syndrome: A systematic review and meta-analysis. *Pediatric dermatology* **37**, 1044-1050 (2020).
965 https://doi.org:10.1111/pde.14326
966 12 Araya, P. *et al.* IGF1 deficiency integrates stunted growth and neurodegeneration in Down
967 syndrome. *Cell reports* **41**, 111883 (2022). https://doi.org:10.1016/j.celrep.2022.111883
968 13 Flores-Aguilar, L. *et al.* Evolution of neuroinflammation across the lifespan of individuals with
969 Down syndrome. *Brain* **143**, 3653-3671 (2020). https://doi.org:10.1093/brain/awaa326
970 14 Wilcock, D. M. & Griffin, W. S. T. Down's syndrome, neuroinflammation, and Alzheimer
971 neuropathogenesis. *Journal of neuroinflammation* **10**, 864 (2013). https://doi.org:10.1186/1742-
972 2094-10-84
973 15 Waugh, K. A. *et al.* Mass Cytometry Reveals Global Immune Remodeling with Multi-lineage
974 Hypersensitivity to Type I Interferon in Down Syndrome. *Cell reports* **29**, 1893-1908 e1894
975 (2019). https://doi.org:10.1016/j.celrep.2019.10.038
976 16 Araya, P. *et al.* Trisomy 21 dysregulates T cell lineages toward an autoimmunity-prone state
977 associated with interferon hyperactivity. *Proc Natl Acad Sci U S A* **116**, 24231-24241 (2019).
978 https://doi.org:10.1073/pnas.1908129116
979 17 Sullivan, K. D. *et al.* Trisomy 21 consistently activates the interferon response. *Elife* **5** (2016).
980 https://doi.org:10.7554/eLife.16220
981 18 Sullivan, K. D. *et al.* Trisomy 21 causes changes in the circulating proteome indicative of
982 chronic autoinflammation. *Scientific reports* **7**, 14818 (2017). https://doi.org:10.1038/s41598-
983 017-13858-3

984 19 Powers, R. K. *et al.* Trisomy 21 activates the kynurenine pathway via increased dosage of
985 interferon receptors. *Nat Commun* **10**, 4766 (2019). https://doi.org:10.1038/s41467-019-12739-9
986 20 Secombes, C. J. & Zou, J. Evolution of Interferons and Interferon Receptors. *Front Immunol* **8**,
987 209 (2017). https://doi.org:10.3389/fimmu.2017.00209
988 21 Waugh, K. A., Minter, R., Baxter, J., Chi, C., Tuttle, K.D., Eduthan, N.P., Galbraith, M.D.,
989 Kinning, K.T., Andrysik, Z., Araya, P., Dougherty, H., Dunn, L.N., Ludwig, M., Schade, K.A.,
990 Tracy, D., Smith, K.P., Granrath, R.E., Busquet, N., Khanal, S., Anderson, R.D., Cox, L.L.,
991 BEnriquez Estrada, B., Rachubinski, A.L., Lyford, H.R., Britton, E.C., Orlicky, D.J., Matsuda,
992 J.L., Song, K., Cox, T.C., Sullivan, K.D., and Espinosa, J.M. Interferon receptor gene dosage
993 determines diverse hallmarks of Down syndrome. *BioRxiv* (2022).
994 https://doi.org:https://doi.org/10.1101/2022.02.03.478982
995 22 Tuttle, K. D. *et al.* JAK1 Inhibition Blocks Lethal Immune Hypersensitivity in a Mouse Model
996 of Down Syndrome. *Cell reports* **33**, 108407 (2020).
997 https://doi.org:10.1016/j.celrep.2020.108407
998 23 Galbraith, M. D., Rachubinski, A.L., Smith, K.P., Araya, P., Waugh, K.A., Enriquez-Estrada, B.,
999 Worek, K., Granrath, R.E., Kinning, K.T., Eduthan, N.P., Ludwig, M.P. Hsieh, E.W.Y., Sullivan,
000 K.D., Espinosa, J.M. Multidimensional definition of the interferonopathy of Down syndrome and
001 its response to JAK inhibition. *Science Advances* **9** (2023).
002 24 Chi, C., Knight, W.E., Riching, A.S., Zhang, Z., Tatavosian, R., Zhuang, Y., Moldovan, R.,
003 Rachubinski, A.L., Gao, D., Xu H., Espinosa, J.M., Song, K. . Interferon hyperactivity impairs
004 cardiogenesis in Down syndrome via downregulation of canonical Wnt signaling. *iScience* **26,**
005 **107012** (2023). https://doi.org:https://doi.org/10.1016/j.isci. 2023.107012
006 25 Lambert, K. *et al.* Deep immune phenotyping reveals similarities between aging, Down
007 syndrome, and autoimmunity. *Science translational medicine* **14**, eabi4888 (2022).
008 https://doi.org:10.1126/scitranslmed.abi4888

009 26 Khor, B. & Buckner, J. H. Down syndrome: insights into autoimmune mechanisms. *Nature*
010 *reviews. Rheumatology*, 1-2 (2023). https://doi.org:10.1038/s41584-023-00970-0
011 27 Gensous, N., Bacalini, M. G., Franceschi, C. & Garagnani, P. Down syndrome, accelerated aging
012 and immunosenescence. *Seminars in immunopathology* (2020). https://doi.org:10.1007/s00281-
013 020-00804-1
014 28 Malle, L. *et al.* Autoimmunity in Down's syndrome via cytokines, CD4 T cells and CD11c(+) B
015 cells. *Nature* **615**, 305-314 (2023). https://doi.org:10.1038/s41586-023-05736-y
016 29 Aversa, T. *et al.* Epidemiological and clinical aspects of autoimmune thyroid diseases in children
017 with Down's syndrome. *Ital J Pediatr* **44**, 39 (2018). https://doi.org:10.1186/s13052-018-0478-9
018 30 Liu, E. *et al.* Routine Screening for Celiac Disease in Children With Down Syndrome Improves
019 Case Finding. *Journal of pediatric gastroenterology and nutrition* **71**, 252-256 (2020).
020 https://doi.org:10.1097/mpg.0000000000002742
021 31 Johnson, M. B. *et al.* Trisomy 21 Is a Cause of Permanent Neonatal Diabetes That Is
022 Autoimmune but Not HLA Associated. *Diabetes* **68**, 1528-1535 (2019).
023 https://doi.org:10.2337/db19-0045
024 32 Aitken, R. J. *et al.* Early-onset, coexisting autoimmunity and decreased HLA-mediated
025 susceptibility are the characteristics of diabetes in Down syndrome. *Diabetes Care* **36**, 1181-
026 1185 (2013). https://doi.org:10.2337/dc12-1712
027 33 Gansa, W. *et al.* Dysregulation of the Immune System in a Natural History Study of 1299
028 Individuals with Down Syndrome. *J Clin Immunol* **44**, 130 (2024).
029 https://doi.org:10.1007/s10875-024-01725-6
030 34 Rakasiwi, T. *et al.* Dermatologic Conditions in Down Syndrome: A Multi-Site Retrospective
031 Review of International Classification of Diseases Codes. *Pediatric dermatology* (2024).
032 https://doi.org:10.1111/pde.15757

033 35 Singh, P. *et al.* Global Prevalence of Celiac Disease: Systematic Review and Meta-analysis. *Clin*
034 *Gastroenterol Hepatol* **16**, 823-836 e822 (2018). https://doi.org:10.1016/j.cgh.2017.06.037
035 36 Markle, J. G. *et al.* Sex differences in the gut microbiome drive hormone-dependent regulation of
036 autoimmunity. *Science* **339**, 1084-1088 (2013). https://doi.org:10.1126/science.1233521
037 37 Molano-Gonzalez, N. *et al.* Cluster analysis of autoimmune rheumatic diseases based on
038 autoantibodies. New insights for polyautoimmunity. *Journal of autoimmunity* **98**, 24-32 (2019).
039 https://doi.org:10.1016/j.jaut.2018.11.002
040 38 Elling, C. L. *et al.* Otitis Media in Children with Down Syndrome Is Associated with Shifts in
041 the Nasopharyngeal and Middle Ear Microbiotas. *Genet Test Mol Biomarkers* **27**, 221-228
042 (2023). https://doi.org:10.1089/gtmb.2023.0132
043 39 Ghazanfari, N., Morsch, M., Reddel, S. W., Liang, S. X. & Phillips, W. D. Muscle-specific
044 kinase (MuSK) autoantibodies suppress the MuSK pathway and ACh receptor retention at the
045 mouse neuromuscular junction. *J Physiol* **592**, 2881-2897 (2014).
046 https://doi.org:10.1113/jphysiol.2013.270207
047 40 Poulter, J. A. *et al.* Novel somatic mutations in UBA1 as a cause of VEXAS syndrome. *Blood*
048 **137**, 3676-3681 (2021). https://doi.org:10.1182/blood.2020010286
049 41 Lin, S. J. *et al.* Biallelic variants in WARS1 cause a highly variable neurodevelopmental
050 syndrome and implicate a critical exon for normal auditory function. *Hum Mutat* **43**, 1472-1489
051 (2022). https://doi.org:10.1002/humu.24435
052 42 Allenbach, Y., Benveniste, O., Stenzel, W. & Boyer, O. Immune-mediated necrotizing
053 myopathy: clinical features and pathogenesis. *Nature reviews. Rheumatology* **16**, 689-701
054 (2020). https://doi.org:10.1038/s41584-020-00515-9
055 43 Amagai, M., Nishikawa, T., Nousari, H. C., Anhalt, G. J. & Hashimoto, T. Antibodies against
056 desmoglein 3 (pemphigus vulgaris antigen) are present in sera from patients with paraneoplastic

057 pemphigus and cause acantholysis in vivo in neonatal mice. *The Journal of clinical investigation*
058 **102**, 775-782 (1998). https://doi.org:10.1172/JCI3647
059 44 Galbraith, M. D. *et al.* Multidimensional definition of the interferonopathy of Down syndrome
060 and its response to JAK inhibition. *Science Advances* **9**, eadg6218 (2023).
061 https://doi.org:doi:10.1126/sciadv.adg6218
062 45 Van Gassen, S. *et al.* FlowSOM: Using self-organizing maps for visualization and interpretation
063 of cytometry data. *Cytometry A* **87**, 636-645 (2015). https://doi.org:10.1002/cyto.a.22625
064 46 Amini, A., Pang, D., Hackstein, C. P. & Klenerman, P. MAIT Cells in Barrier Tissues: Lessons
065 from Immediate Neighbors. *Front Immunol* **11**, 584521 (2020).
066 https://doi.org:10.3389/fimmu.2020.584521
067 47 Zhang, Y. *et al.* Aberrations in circulating inflammatory cytokine levels in patients with Down
068 syndrome: a meta-analysis. *Oncotarget* **8**, 84489-84496 (2017).
069 https://doi.org:10.18632/oncotarget.21060
070 48 Kusters, M. A., Gemen, E. F., Verstegen, R. H., Wever, P. C. & E, D. E. V. Both normal
071 memory counts and decreased naive cells favor intrinsic defect over early senescence of Down
072 syndrome T lymphocytes. *Pediatr Res* **67**, 557-562 (2010).
073 https://doi.org:10.1203/PDR.0b013e3181d4eca3
074 49 Trotta, M. B. *et al.* Inflammatory and Immunological parameters in adults with Down syndrome.
075 *Immun Ageing* **8**, 4 (2011). https://doi.org:10.1186/1742-4933-8-4
076 50 Waugh, K. A. *et al.* Triplication of the interferon receptor locus contributes to hallmarks of
077 Down syndrome in a mouse model. *Nature genetics* (2023). https://doi.org:10.1038/s41588-023-
078 01399-7
079 51 Rachubinski, A. L. *et al.* Janus kinase inhibition in Down syndrome: 2 cases of therapeutic
080 benefit for alopecia areata. *JAAD Case Rep* **5**, 365-367 (2019).
081 https://doi.org:10.1016/j.jdcr.2019.02.007

082 52 Pham, A. T. *et al.* JAK inhibition for treatment of psoriatic arthritis in Down syndrome.
083 *Rheumatology* (2021). https://doi.org:10.1093/rheumatology/keab203
084 53 Guild, A., Fritch, J., Patel, S., Reinhardt, A. & Acquazzino, M. Hemophagocytic
085 lymphohistocytosis in trisomy 21: successful treatment with interferon inhibition. *Pediatr*
086 *Rheumatol Online J* **20**, 104 (2022). https://doi.org:10.1186/s12969-022-00764-w
087 54 Cohen, S. B. *et al.* Long-term safety of tofacitinib for the treatment of rheumatoid arthritis up to
088 8.5 years: integrated analysis of data from the global clinical trials. *Ann Rheum Dis* **76**, 1253-
089 1262 (2017). https://doi.org:10.1136/annrheumdis-2016-210457
090 55 Honda, K., Takaoka, A. & Taniguchi, T. Type I interferon [corrected] gene induction by the
091 interferon regulatory factor family of transcription factors. *Immunity* **25**, 349-360 (2006).
092 https://doi.org:10.1016/j.immuni.2006.08.009
093 56 Schwartz, D. M. *et al.* JAK inhibition as a therapeutic strategy for immune and inflammatory
094 diseases. *Nature reviews. Drug discovery* **17**, 78 (2017). https://doi.org:10.1038/nrd.2017.267
095 57 Schwartz, D. M., Bonelli, M., Gadina, M. & O'Shea, J. J. Type I/II cytokines, JAKs, and new
096 strategies for treating autoimmune diseases. *Nature reviews. Rheumatology* **12**, 25-36 (2016).
097 https://doi.org:10.1038/nrrheum.2015.167
098 58 Maroun, L. E., Heffernan, T. N. & Hallam, D. M. Partial IFN-alpha/beta and IFN-gamma
099 receptor knockout trisomy 16 mouse fetuses show improved growth and cultured neuron
100 viability. *Journal of interferon & cytokine research : the official journal of the International*
101 *Society for Interferon and Cytokine Research* **20**, 197-203 (2000).
102 https://doi.org:10.1089/107999000312612
103 59 Bhattacharya, S., Cherry, C., Deutsch, G., Birth Defects Research Laboratory (BDRL), Glass,
104 I.A., Mariani, T.J., Al Alam, D., Danopoulos, S. A Trisomy 21 Lung Cell Atlas. *bioRxiv* **doi:**
105 **https://doi.org/10.1101/2023.03.30.534839** (2023). https://doi.org:doi:
106 https://doi.org/10.1101/2023.03.30.534839

107 60 Aziz, N. M. *et al.* Lifespan analysis of brain development, gene expression and behavioral
108 phenotypes in the Ts1Cje, Ts65Dn and Dp(16)1/Yey mouse models of Down syndrome. *Dis*
109 *Model Mech* **11** (2018). https://doi.org:10.1242/dmm.031013
110 61 Rodero, M. P. & Crow, Y. J. Type I interferon-mediated monogenic autoinflammation: The type
111 I interferonopathies, a conceptual overview. *The Journal of experimental medicine* **213**, 2527-
112 2538 (2016). https://doi.org:10.1084/jem.20161596
113 62 Breslin, N. K., Varadarajan, V. V., Sobel, E. S. & Haberman, R. S. Autoimmune inner ear
114 disease: A systematic review of management. *Laryngoscope Investig Otolaryngol* **5**, 1217-1226
115 (2020). https://doi.org:10.1002/lio2.508
116 63 Kocyigit, M. *et al.* Association Between Endocrine Diseases and Serous Otitis Media in
117 Children. *J Clin Res Pediatr Endocrinol* **9**, 48-51 (2017). https://doi.org:10.4274/jcrpe.3585
118 64 Ercolini, A. M. & Miller, S. D. The role of infections in autoimmune disease. *Clin Exp Immunol*
119 **155**, 1-15 (2009). https://doi.org:10.1111/j.1365-2249.2008.03834.x
120 65 Dresser, L., Wlodarski, R., Rezania, K. & Soliven, B. Myasthenia Gravis: Epidemiology,
121 Pathophysiology and Clinical Manifestations. *J Clin Med* **10** (2021).
122 https://doi.org:10.3390/jcm10112235
123 66 Shawky, A. M., Almalki, F. A., Abdalla, A. N., Abdelazeem, A. H. & Gouda, A. M. A
124 Comprehensive Overview of Globally Approved JAK Inhibitors. *Pharmaceutics* **14** (2022).
125 https://doi.org:10.3390/pharmaceutics14051001
126 67 Ruperto, N. *et al.* Tofacitinib in juvenile idiopathic arthritis: a double-blind, placebo-controlled,
127 withdrawal phase 3 randomised trial. *Lancet* **398**, 1984-1996 (2021).
128 https://doi.org:10.1016/S0140-6736(21)01255-1
129 68 King, B. A. & Craiglow, B. G. Janus kinase inhibitors for alopecia areata. *Journal of the*
130 *American Academy of Dermatology* **89**, S29-S32 (2023).
131 https://doi.org:10.1016/j.jaad.2023.05.049

132 69 Tampa, M., Mitran, C. I., Mitran, M. I. & Georgescu, S. R. A New Horizon for Atopic
133 Dermatitis Treatments: JAK Inhibitors. *J Pers Med* **13** (2023).
134 https://doi.org:10.3390/jpm13030384
135 70 Ytterberg, S. R. *et al.* Cardiovascular and Cancer Risk with Tofacitinib in Rheumatoid Arthritis.
136 *The New England journal of medicine* **386**, 316-326 (2022).
137 https://doi.org:10.1056/NEJMoa2109927
138 71 Santoro, J. D. *et al.* Assessment and Diagnosis of Down Syndrome Regression Disorder:
139 International Expert Consensus. *Front Neurol* **13**, 940175 (2022).
140 https://doi.org:10.3389/fneur.2022.940175
141 72 Harris, P. A. *et al.* Research electronic data capture (REDCap)--a metadata-driven methodology
142 and workflow process for providing translational research informatics support. *J Biomed Inform*
143 **42**, 377-381 (2009). https://doi.org:10.1016/j.jbi.2008.08.010
144 73 Gu, Y. *et al.* High-throughput multiplexed autoantibody detection to screen type 1 diabetes and
145 multiple autoimmune diseases simultaneously. *EBioMedicine* **47**, 365-372 (2019).
146 https://doi.org:10.1016/j.ebiom.2019.08.036
147 74 Finck, R. *et al.* Normalization of mass cytometry data with bead standards. *Cytometry A* **83**, 483-
148 494 (2013). https://doi.org:10.1002/cyto.a.22271
149 75 Zunder, E. R. *et al.* Palladium-based mass tag cell barcoding with a doublet-filtering scheme and
150 single-cell deconvolution algorithm. *Nature protocols* **10**, 316-333 (2015).
151 https://doi.org:10.1038/nprot.2015.020
152 76 Hahne, F. *et al.* flowCore: a Bioconductor package for high throughput flow cytometry. *BMC*
153 *bioinformatics* **10**, 106 (2009). https://doi.org:10.1186/1471-2105-10-106
154 77 Chevrier, S. *et al.* Compensation of Signal Spillover in Suspension and Imaging Mass
155 Cytometry. *Cell Syst* **6**, 612-620 e615 (2018). https://doi.org:10.1016/j.cels.2018.02.010

156 78 Azad, A., Rajwa, B. & Pothen, A. flowVS: channel-specific variance stabilization in flow
157 cytometry. *BMC Bioinformatics* **17**, 291 (2016). https://doi.org:10.1186/s12859-016-1083-9
158 79 Love, M. I., Huber, W. & Anders, S. Moderated estimation of fold change and dispersion for
159 RNA-seq data with DESeq2. *Genome biology* **15**, 550 (2014). https://doi.org:10.1186/s13059-
160 014-0550-8
161 80 Subramanian, A. *et al.* Gene set enrichment analysis: a knowledge-based approach for
162 interpreting genome-wide expression profiles. *Proc Natl Acad Sci U S A* **102**, 15545-15550
163 (2005). https://doi.org:10.1073/pnas.0506580102
164 81 de Jesus, A. A. *et al.* Distinct interferon signatures and cytokine patterns define additional
165 systemic autoinflammatory diseases. *The Journal of clinical investigation* **130**, 1669-1682
166 (2020). https://doi.org:10.1172/JCI129301
167 82 Banchereau, R. *et al.* Personalized Immunomonitoring Uncovers Molecular Networks that
168 Stratify Lupus Patients. *Cell* **165**, 1548-1550 (2016). https://doi.org:10.1016/j.cell.2016.05.057
169
170

171 **Article and author information.**

172 **Acknowledgements:** This work was supported primarily by NIH grant R61AR077495. Additional
173 funding was provided by NIH grants R01AI150305 (J.M.E.), T32CA190216 (K.A.W.), 2T32AR007411-
174 31 (K.A.W.), UM1TR004399 (data generation and REDCap support), P30CA046934 (support of shared
175 resources), the Linda Crnic Institute for Down Syndrome, the Global Down Syndrome Foundation, the
176 Anna and John J. Sie Foundation, the Human Immunology and Immunotherapy Initiative, the University
177 of Colorado School of Medicine, the Boettcher Foundation, and Fast Grants. We are grateful to all research
178 participants and their families involved in the Human Trisome Project and the clinical trial. We thank
179 Lyndy Bush for administrative support, Dr. Kim Jordan and her team at the Human Immune Monitoring
180 Shared Resource for outstanding service in generation of the immune marker dataset, and Dr. Eric
181 Clambey and his team at the Flow Cytometry Shared Resource for outstanding service in generation of
182 the mass cytometry dataset. We are also grateful to the Colorado Translational and Sciences Institute and
183 the Colorado Multiple Institutional Review Board for assistance in all clinical research projects involving
184 the Crnic Institute. Special thanks to Michelle Sie Whitten, the team at the Global Down Syndrome
185 Foundation, Dr. John Reilly, and Dr. Ron Sokol for logistical support at multiple stages of the project.

186

187 **Author Contributions Statement:** A.L.R.: conceptualization, methodology, formal analysis, project
188 administration, data curation, visualization, investigation, resources, writing of manuscript; E.W.:
189 methodology, data curation, investigation, writing of manuscript; E.G.: methodology, data curation,
190 investigation, writing of manuscript; BEE: methodology, project administration, data curation,
191 investigation, writing of manuscript; K.R.W.: methodology, data curation, investigation, writing of
192 manuscript; K.P.S.: methodology, project administration, formal analysis, data curation, visualization,
193 investigation, writing of manuscript; P.A.: conceptualization, methodology, formal analysis, data curation,
194 visualization, investigation, writing of manuscript; K.A.W.: conceptualization, methodology,

investigation, writing of manuscript; R.E.G.: methodology, investigation, writing of manuscript; E.B.: methodology, investigation, writing of manuscript; H.R.L.: methodology, investigation, writing of manuscript; M.G.D.: methodology, investigation, formal analysis, data curation, visualization, writing of manuscript; N.P.E.: methodology, investigation, formal analysis, data curation, visualization, writing of manuscript; A.A.H.: conceptualization, methodology, project administration, investigation, writing of manuscript; B.M.: methodology, data curation, investigation, writing of manuscript; K.D.S.: methodology, investigation, visualization, writing of manuscript; L.P.: methodology, investigation, formal analysis, data curation, project administration, writing of manuscript; D.F.: methodology, investigation, formal analysis, data curation, project administration, writing of manuscript; M.D.G.: methodology, investigation, formal analysis, data curation, visualization, project administration, writing of manuscript; C.A.D.: conceptualization, methodology, data curation, investigation, project administration, writing of manuscript; D.A.N.: conceptualization, methodology, data curation, investigation, resources, project administration, writing of manuscript; J.M.E.: conceptualization, methodology, project administration, visualization, investigation, resources, writing of manuscript.

Competing Interests Statement: J.M.E. has provided consulting services for Eli Lilly Co., Gilead Sciences Inc., and Biohaven Pharmaceuticals and serves on the advisory board of Perha Pharmaceuticals. The remaining authors declare no competing interests.

214 **Supplementary File Legends.**

215 **Supplementary file 1.** (A) Cohort characteristics and (B) clinical data for Human Trisome Project
216 participants analyzed in this study.

217 **Supplementary file 2.** Autoantibody measurements of Human Trisome Project participants: (A) anti-
218 thyroid peroxidase (TPO) reactivity; (B) anti-nuclear antigen (ANA) reactivity; (C) SciLifeLabs
219 autoantigen peptide array data.

220 **Supplementary file 3.** (A) Minimum qualifying scores for skin conditions. (B) Cohort characteristics for
221 clinical trial participants.

222 **Supplementary file 4.** Adverse events for clinical trial participants.

223 **Supplementary file 5.** Skin pathology metrics for clinical trial participants: (A) Investigator's Global
224 Assessment (IGA); (B) Dermatology Life Quality Index (DLQI); (C) Severity of Alopecia Tool (SALT);
225 (D) Psoriasis Area and Severity Index (PASI); and (E) Eczema Area and Severity Index (EASI).

226 **Supplementary file 6.** (A) DS IFN scores; (B) Cytokine scores; (C) anti-thyroid peroxidase (TPO) titers;
227 (D) anti-transglutaminase (TG) titers; and (E) anti-thyroid stimulating hormone receptor (TSHR) titers for
228 clinical trial participants.

229 **Supplementary file 7.** Marker information for mass cytometry analysis.

230 **Supplementary file 8.** Clinical trial protocol.

231

232